

AD-A039 656

TETRA TECH INC PASADENA CALIF

F/G 20/14

PARAMETER STUDY OF REFLECTION REDUCTION BY IMPEDANCE GRIDS. (U)

SEP 75 R W LATHAM

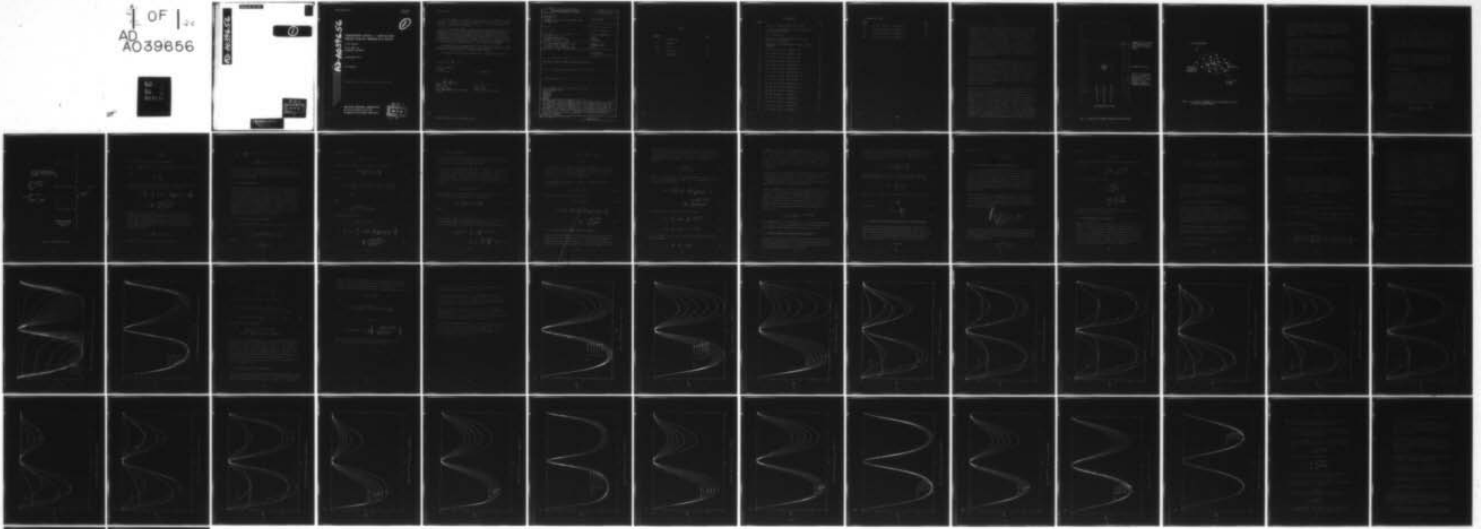
F29601-72-C-0089

UNCLASSIFIED

AFWL-TR-74-69

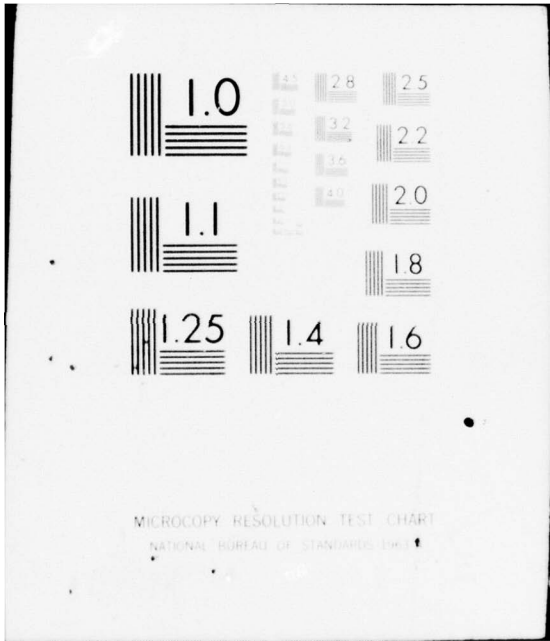
NL

1 OF 1
AD
A039656



END

DATE
FILMED
6-77



4 D D C
RECEIVED
MAY 19 1977
D

DISTRIBUTION STATEMENT A

Approved for public release;
Distribution Unlimited

AD-A039656



PARAMETER STUDY OF REFLECTION REDUCTION BY IMPEDANCE GRIDS

R. W. Latham
Tetra Tech, Inc.
Pasadena, CA 91107

September 1975

Final Report

Approved for public release; distribution unlimited.

AIR FORCE WEAPONS LABORATORY
Air Force Systems Command
Kirtland Air Force Base, NM 87117



This final report was prepared by the Tetra Tech, Inc., Pasadena, California, under Contract F29601-72-C-0089, Job Order 46950305 with the Air Force Weapons Laboratory, Kirtland Air Force Base, New Mexico. Lt. M. G. Harrison was the Laboratory Project Officer-in-Charge.

When US Government drawings, specifications, or other data are used for any purpose other than a definitely related Government procurement operation, the Government thereby incurs no responsibility nor any obligation whatsoever, and the fact that the Government may have formulated, furnished, or in any way supplied the said drawings, specifications, or other data is not to be regarded by implication or otherwise as in any manner licensing the holder or any other person or corporation or conveying any rights or permission to manufacture, use, or sell any patented invention that may in any way be related thereto.

This report has been reviewed by the Information Office (OI) and is releasable to the National Technical Information Service (NTIS). At NTIS, it will be available to the general public, including foreign nations.

This technical report has been reviewed and is approved for publication.

Michael G. Harrison

MICHAEL G. HARRISON
LT., USAF
Project Officer

FOR THE COMMANDER

Larry W. Wood

LARRY W. WOOD
Lt. Colonel, USAF
Chief, Phenomenology and Technology
Branch

John W. Swan

JOHN W. SWAN
Colonel, USAF
Chief, Electronics Division

REPORT DOCUMENTATION PAGE		READ INSTRUCTIONS BEFORE COMPLETING FORM
1. REPORT NUMBER AFWL-TR-74-69	2. GOVT ACCESSION NO.	3. RECIPIENT'S CATALOG NUMBER
4. TITLE (and Subtitle) PARAMETER STUDY OF REFLECTION REDUCTION BY IMPEDANCE GRIDS	5. TYPE OF REPORT & PERIOD COVERED Final Report	
	6. PERFORMING ORG. REPORT NUMBER	
7. AUTHOR(s) R. W. Latham	8. CONTRACT OR GRANT NUMBER(s) F29601-72-C-0089	
9. PERFORMING ORGANIZATION NAME AND ADDRESS Tetra Tech, Inc. 630 North Rosemead Blvd Pasadena, California 91107	10. PROGRAM ELEMENT, PROJECT, TASK AREA & WORK UNIT NUMBERS 64711F 46950305	
11. CONTROLLING OFFICE NAME AND ADDRESS Air Force Weapons Laboratory (ELP) Air Force Systems Command Kirtland Air Force Base, NM 87117	12. REPORT DATE September 1975	
	13. NUMBER OF PAGES 54	
14. MONITORING AGENCY NAME & ADDRESS (if different from Controlling Office)	15. SECURITY CLASS. (of this report) Unclassified	
	15a. DECLASSIFICATION/DOWNGRADING SCHEDULE	
16. DISTRIBUTION STATEMENT (of this Report) Approved for public release; distribution unlimited.		
17. DISTRIBUTION STATEMENT (of the abstract entered in Block 20, if different from Report)		
18. SUPPLEMENTARY NOTES		
19. KEY WORDS (Continue on reverse side if necessary and identify by block number) Electromagnetic Field Satellite Impedance Reflection Chamber		
20. ABSTRACT (Continue on reverse side if necessary and identify by block number) Electromagnetic reflection from the walls of the vacuum chamber of a satellite simulator may be reduced by placing one or more grids of wires having known impedances just inside the conducting wall. This report presents the results of a parameter study on the effect of wire spacing and wire resistance and inductance on the frequency dependence of the reflection coefficient of a wall with such a grid in front of it. This data should be useful in helping to choose good values of the design parameters of reflection reducing grids in satellite simulators.		

CONTENTS

<u>SECTION</u>		<u>PAGE</u>
I	INTRODUCTION	3
II	ANALYSIS	7
III	DATA	26
IV	DISCUSSION	48
	REFERENCES	51

ILLUSTRATIONS

<u>Figure</u>		<u>Page</u>
1	Scheme of a System Generated EMP Simulator	4
2	3-D Array of Admittances for Reflection Reduction and Damping of Resonance	5
3	The N-Grid Problem	8
4	Inductive - Resistive Null Sheets for Various Values of D/λ_0 ($=k_0 D/2\pi$)	22
5	Approximate Nulls Resulting from Varying L_w Only ($R_w = Z_0/d$)	23
6	$ R ^2$ vs. D/λ for $z_r = 1$ and $d/a = 20$	27
7	$ R ^2$ vs. D/λ for $z_r = 1$ and $d/a = 100$	28
8	$ R ^2$ vs. D/λ for $z_r = 1$ and $d/a = 500$	29
9	$ R ^2$ vs. D/λ for $d/a = 20$ and $d/D = 1$	30
10	$ R ^2$ vs. D/λ for $d/a = 20$ and $d/D = .5$	31
11	$ R ^2$ vs. D/λ for $d/a = 20$ and $d/D = .1$	32
12	$ R ^2$ vs. D/λ for $f/a = 100$ and $d/D = 1$	33
13	$ R ^2$ vs. D/λ for $d/a = 100$ and $d/D = .5$	34
14	$ R ^2$ vs. D/λ for $d/a = 100$ and $d/D = .1$	35
15	$ R ^2$ vs. D/λ for $d/a = 500$ and $d/D = 1$	36
16	$ R ^2$ vs. D/λ for $d/a = 500$ and $d/D = .5$	37
17	$ R ^2$ vs. D/λ for $d/a = 500$ and $d/D = .1$	38
18	$ R ^2$ vs. D/λ for $z_r = .5$ and $d/D = 1$	39
19	$ R ^2$ vs. D/λ for $z_r = .5$ and $d/D = .5$	40
20	$ R ^2$ vs. D/λ for $z_r = .5$ and $d/D = .1$	41
21	$ R ^2$ vs. D/λ for $z_r = 1$ and $d/D = 1$	42
22	$ R ^2$ vs. D/λ for $z_r = 1$ and $d/D = .5$	43

Illustrations (cont.)

<u>Figure</u>		<u>Page</u>
23	$ R ^2$ vs. D/λ for $z_r = 1$ and $d/D = .1$	44
24	$ R ^2$ vs. D/λ for $z_r = 2$ and $d/D = 1$	45
25	$ R ^2$ vs. D/λ for $z_r = 2$ and $d/D = .5$	46
26	$ R ^2$ vs. D/λ for $z_r = 2$ and $d/D = .1$	47

SECTION I
INTRODUCTION

A general technique for simulating the system generated electromagnetic pulse resulting from an exoatmospheric nuclear weapon radiation environment has been described in a previous note in this series [1]. The general form that a simulator would take, if its design were based on this technique, is shown in Fig. 1, taken from Ref. [1]. The region of sparse wires with resistors to absorb electromagnetic energy, shown only symbolically in Fig. 1, is shown semi-realistically in Fig. 2, which is also taken from Ref. [1]. In this note we will be interested only in the reflection reduction properties of such a grid. Resonance damping properties are a separate subject which has been, and will be, considered elsewhere by other workers.

Since our sole concern here is with reflection reduction, we are primarily concerned with the higher frequencies of the electromagnetic pulse generated by the system under test. This in turn implies that the exact shape of the wall of the vacuum enclosure makes very little difference, and that we can get a very good estimate of the reflection reducing properties of any particular grid by assuming the wall to be an infinite conducting plane and the grid to be an infinite periodic structure in front of the plane. Figure 2 can also be considered as a representation of a small portion of this infinite plane structure.

We will make one further basic assumption in our treatment of reflection reduction. Since the actual generator of the electromagnetic pulse, i. e. the system under test, will be rather small compared to the size of the vacuum chamber, and since the vacuum chamber will be approximately spherical, most of the high frequency electromagnetic energy that reaches the walls will be almost normally incident. Accordingly, we will not vary the angle of incidence in our parameter studies; all waves will be normally incident. The assumption of normal incidence has an additional benefit besides restricting the parameter study. This assumption greatly simplifies the calculational problem, the reason being that at normal incidence the coupling between the perpendicular sets of wires in the grid

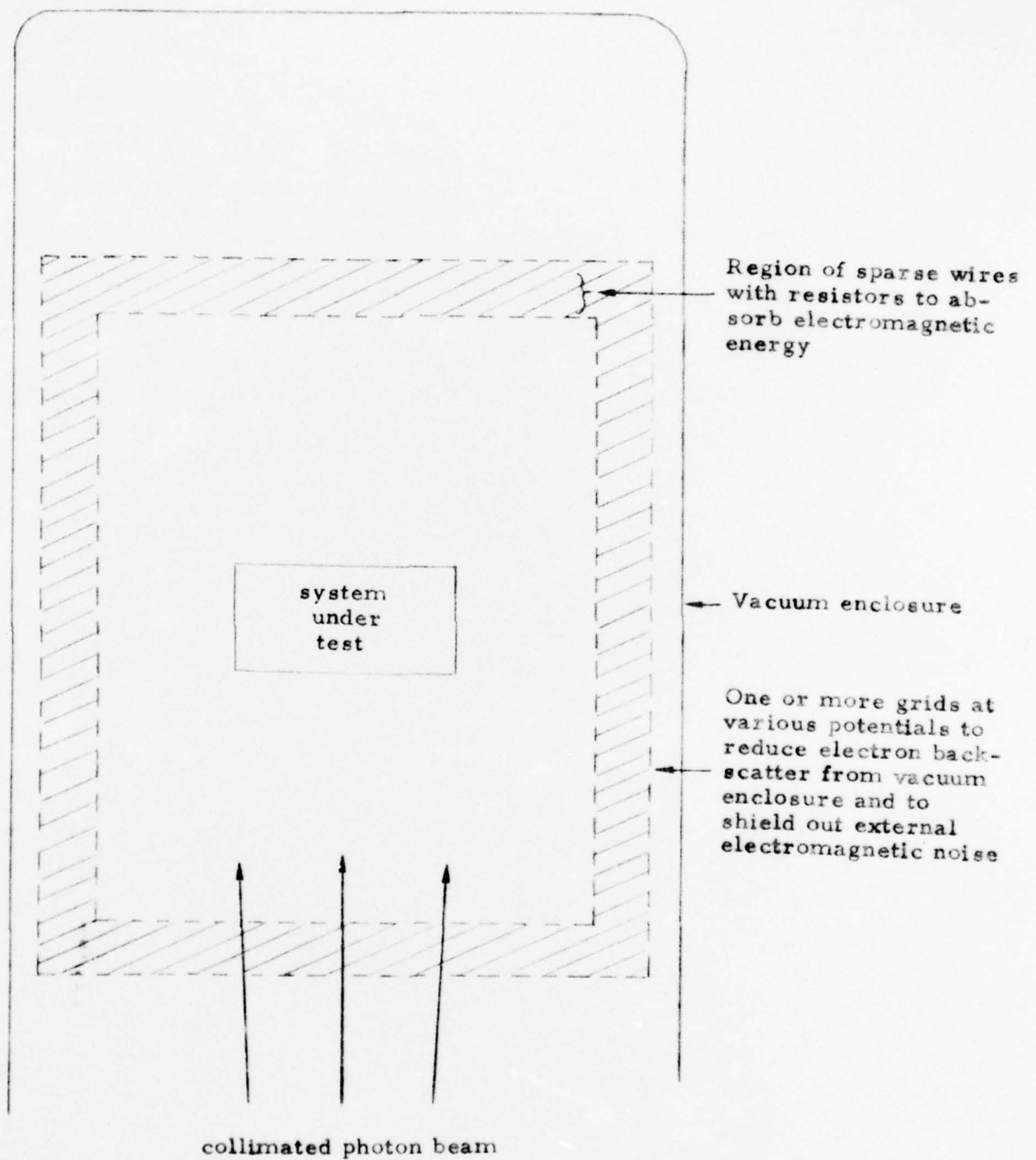


Fig. 1: Scheme of a System Generated EMP Simulator

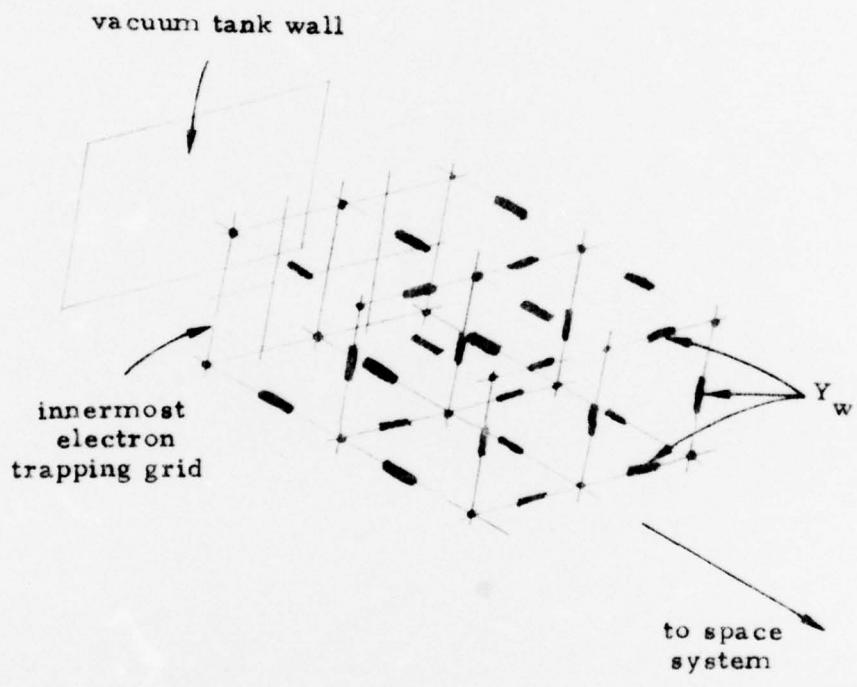


Fig. 2: 3-D Array of Admittances for Reflection Reduction and Damping of Resonance

becomes quite small (disappearing in the limit of small wire radius), and so this coupling can be neglected. An analytical demonstration of this decoupling of wire sets at normal incidence (although it should clearly be the case on physical grounds) has appeared in the recent open literature [2].

We are left, then, with the problem of calculating the reflection coefficient of a plane wave normally incident on a perfectly conducting plane when there are one or more impedance-loaded parallel-wire grids in front of the plane. Because of the above mentioned decoupling, it is sufficient to consider the electric field of the incident wave to be parallel to the wires of the grids.

One analytical treatment of the single resistive grid problem was published twenty years ago by Wait [3]. We will extend these results to the case of several parallel grids of arbitrary internal impedance and derive an effective distance from the plane of an equivalent uniform sheet in the case of a single grid. This analytical work, based on an approach slightly different from that of Wait, is presented in Section II.

But the main purpose of the present note is to present the parameter study of Section III. In this study, we will vary the spacing, radius, resistance and inductance of the wires of the grid and plot the reflection coefficient of the grid-plane system as a function of frequency. Enough values of the various parameters will be given that a good idea of what can be accomplished with a single grid will become evident.

In the last section we will give a brief discussion of the data presented in Section III.

SECTION II

ANALYSIS

The structure we wish to analyze is shown in Fig. 3. One or more parallel-wire grids are placed in front of a perfectly conducting plane. A plane wave, whose electric vector is parallel to the wires of the grids, is normally incident on the structure. We wish to calculate the fraction of the incident energy that is reflected, as a function of frequency. The parameters of the problem are the spacing between wires in a grid, the radius and impedance of an individual grid wire, and the spacing between grids.

We will first formulate the general problem, then specialize to the case of one grid, then discuss several topics having to do with the uniform sheet approximation to a single grid, and finally go into a little more detail on the meaning of the equations for the single grid case.

II.A. General Approach

In a previous note [4] we have discussed the reflection of a plane wave from N rows of dielectric posts. In that note the posts were characterized by an impedance per unit length, Z_p . The present problem would be almost identical to the previous one if the conducting plane were removed. The only difference would be the different orders of magnitude of Z_p and Z_w . This makes no difference to the algebra. Thus from the work of Ref. [4] we can say (there are slight changes in the appearance of the equations since we are now numbering the rows backwards from the origin rather than forward), if the conducting plane were not present and if all D 's were equal (this restriction on the D 's is not necessary, but it simplifies the following formulae),

$$\left| R_N \right| = \frac{1}{2} \left| \sum_{n=1}^N X_n e^{inkD} \right| \quad (1)$$

where the X_n , defined by

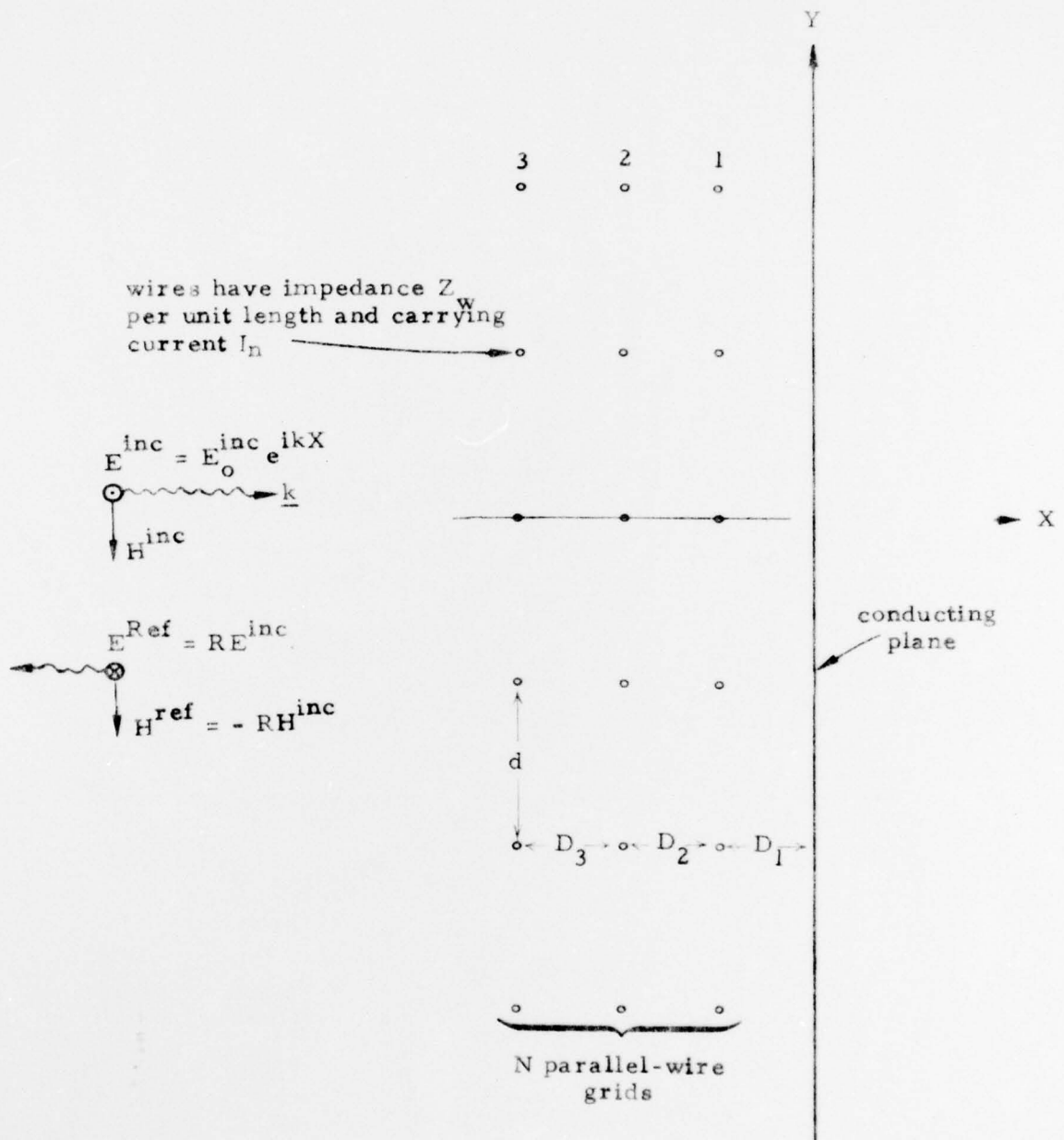


Fig. 3: The N-Grid Problem

$$X_n \equiv \frac{Z_{o n}^1}{d E_o^{\text{inc}}} , \quad (2)$$

are to be found from the solution of the equations

$$z_w^n X_n + \frac{1}{2} \sum_{m=1}^N e^{ikD|n-m|} X_m = e^{-inkD} + \frac{1}{2} \sum_{m=1}^N P_{|n-m|} X_m \quad [1 \leq n \leq N] \quad (3)$$

where

$$z_w^n \equiv \frac{Z_w^n d}{Z_o} , \quad (4)$$

i. e. the wires within a single grid are equivalent, although there may be variations from grid to grid. The P_n of Eqs. 3 are defined by

$$P_o = \frac{d}{\lambda} \left\{ \pi + 2i \left[\gamma + \ell n \left(\frac{d}{2\lambda} \right) + \sum_{n=1}^{\infty} \left(\frac{1}{\sqrt{n^2 - (d/\lambda)^2}} - \frac{1}{n} \right) \right] \right\} \quad (5)$$

$$P_n = 2i \sum_{m=1}^{\infty} \frac{e^{-nkD} \sqrt{(m\lambda/d)^2 - 1}}{\sqrt{(m\lambda/d)^2 - 1}} , \quad n > 0 \quad (6)$$

Now the presence of the conducting plane in the problem at hand can be taken into account by adding the wave reflected from the plane (with no grids present) to the forcing term of Eqs. 3, and at the same time adding negative image currents at the image position (with respect to the conducting plane) of each grid wire. This results in the reflection coefficient now being given by

$$R = -1 + i \sum_{n=1}^N X_n \sin(nkD) \quad (7)$$

where the X_n are now given by the solution of the set

$$z_w^n X_n + \frac{1}{2} \sum_{m=1}^N \left(e^{i|n-m|kD} - e^{i|n+m|kD} \right) X_m = -2i \sin nkD + \frac{1}{2} \sum_{m=1}^N \left(P_{|n-m|} - P_{n+m} \right) X_m \quad [1 \leq n \leq N] \quad (8)$$

Equations 7 and 8 constitute the general formulation of the reflection reducing grid problem. In the following subsections we will study particular cases and approximations in order to get a feeling for just what can be expected from such a grid.

II. B The Single Grid Case

The major simplification we will impose on Eqs. 8 is that, in the present note, we will consider only the case where N is one. This allows us to write down reasonably simple explicit solutions and to give a detailed study of the effect of wire spacing and wire impedance. Such a grid would also, of course, be the easiest to construct. Should the single-grid reflection reducer prove inadequate for satellite simulators, a numerical study of Eqs. 7 and 8 could be performed at some later time. It is felt, however, that the single-grid reducer may be good enough, or at least that the gains to be obtained from extra grids may not be enough to make up for the additional complexity of the construction.

If N is unity, Eq. 8 reduces immediately to

$$z_w X_1 + \frac{1}{2} \left(1 - e^{2ikD} \right) X_1 = -2i \sin kD + \frac{1}{2} \left(P_0 - P_2 \right) X_1 \quad (9)$$

i. e.

$$X_1 = \frac{-2i \sin kD}{z_w - ie^{ikD} \sin kD - \frac{1}{2} \left(P_0 - P_2 \right)} \quad (10)$$

and so

$$R = -1 + \frac{2 \sin^2 kD}{z - ie^{ikD} \sin kD} \quad (11)$$

where we have defined

$$z = z_w - \frac{1}{2} (P_0 - P_2) = z_r + iz_i \quad (12)$$

Some simple manipulations of Eq. 11 change it to the form

$$R = e^{-2ikD} \left\{ \frac{-ze^{ikD} + i \sin kD}{ze^{-ikD} - i \sin kD} \right\} \quad (13)$$

and so

$$|R|^2 = \frac{\sin^2 kD + |z|^2 - 2 \sin kD (z_r \sin kD + z_i \cos kD)}{\sin^2 kD + |z|^2 + 2 \sin kD (z_r \sin kD - z_i \cos kD)} \quad (14)$$

$$= \frac{1 - \alpha}{1 + \alpha} \quad (15)$$

where

$$\alpha = \frac{2z_r \sin^2 kD}{\sin^2 kD + |z|^2 - z_i \sin 2kD} \quad (16)$$

and, from Eqs. 4, 5, 6 and 12

$$z_r = \frac{d}{Z_0} \operatorname{Re} Z_w - \frac{\pi}{2} (d/\lambda) \quad (17)$$

$$z_i = \frac{d}{Z_0} \operatorname{Im} Z_w - \frac{d}{\lambda} \left[\gamma + \ln \left(\frac{d}{2\lambda} \right) + \sum_{n=1}^{\infty} \left(\frac{1}{\sqrt{n^2 - (d/\lambda)^2}} - \frac{1}{n} \right) \right] \\ + \sum_{n=1}^{\infty} \frac{e^{-2nkD} \sqrt{(n\lambda/d)^2 - 1}}{\sqrt{(n\lambda/d)^2 - 1}} \quad (18)$$

II. C A Closer Examination of z

Before we proceed further, it is necessary to give a more precise meaning to the quantity we have designated as Z_w , and thus to give a more precise meaning to the z defined in the previous section.

Actually, from the derivations in Ref. [4], it is clear that Z_w is the total impedance per unit length of the grid wires, including both "internal" and "external" impedances per unit length. The "external" impedance of the wire is the impedance of a perfectly conducting wire of the same radius. If the wire is circular, of radius "a", this "external" impedance is easily shown to be

$$Z_w^{\text{ext}} = \frac{kZ_o}{4} H_o^{(1)}(ka) \quad (19)$$

where $H_o^{(1)}(ka)$ is the cylindrical Hankel function of order zero. For the sizes of wire we are talking about, Eq. 19 reduces to

$$Z_w^{\text{ext}} = \frac{kZ_o}{4} \left[1 + \frac{2i}{\pi} \ln\left(\frac{\Gamma ka}{2}\right) \right] \quad (20)$$

where

$$\Gamma = e^{\gamma} = 1.77+. \quad (21)$$

The real part of Z_w^{ext} is the radiation resistance per unit length of wire. It is independent of the exact shape of the wire's cross-section (as long as this cross-section is small), as can be seen by the little calculation

$$\begin{aligned} R_e \left(Z_w^{\text{ext}} \right) |I|^2 &= \lim_{r \rightarrow \infty} \frac{1}{Z_o} \int_0^{2\pi} |E^{\text{rad}}|^2 r d\varphi \\ &= \lim_{r \rightarrow \infty} \frac{1}{Z_o} \frac{\omega^2 \mu_o^2 |I|^2}{16} \int_0^{2\pi} |H_o^{(1)}(kr)|^2 r d\varphi \end{aligned}$$

$$\begin{aligned}
&= \frac{1}{Z_0} \frac{\omega^2 \mu_0^2 |I|^2}{16} \cdot \frac{2}{\pi k} \cdot 2\pi \\
&= |I|^2 \frac{kZ_0}{4}
\end{aligned}$$

The imaginary part of Z_w^{ext} does depend to a slight extent on the shape of the wire's cross section, but there will always be some "equivalent" radius, and, since this equivalent radius appears only as an argument of a ℓn , its exact value is fairly unimportant.

It is now clear that if we write Z_w as the sum of the internal and external impedances, i. e. if

$$Z_w = Z_w^{\text{int}} + Z_w^{\text{ext}}, \quad (22)$$

then from Eqs. 17, 18 and 20 it follows that

$$z_r = \frac{d}{Z_0} \operatorname{Re} Z_w^{\text{int}} \quad (23)$$

$$\begin{aligned}
z_i = \frac{d}{Z_0} \operatorname{Im} Z_w^{\text{int}} - \frac{d}{\lambda} \left[\ell n \left(\frac{d}{2\pi a} \right) + \sum_{n=1}^{\infty} \left(\frac{1}{\sqrt{n^2 - (d/\lambda)^2}} - \frac{1}{n} \right) \right] \\
+ \sum_{n=1}^{\infty} \frac{e^{-2nkD\sqrt{(n\lambda/d)^2 - 1}}}{\sqrt{(n\lambda/d)^2 - 1}} \quad (24)
\end{aligned}$$

II. D Equivalent Uniform Sheet Reflection Reducers

The effect of the discreteness of the wires making up the grid makes the above equations look a little messy. It would be nice if one could design a reflection reducer by assuming it to be a uniform sheet, imposing the fact that it is actually constructed of a set of wires by a slight subsequent

adjustment of the distance of the wires from the conducting plane or a slight change in a parameter of the uniform sheet. This distance adjustment method proves to be possible if we restrict our attention to the very low frequency (small kD) region. In that case α , as given by Eq. 16, reduces to

$$\alpha = \frac{2z_r (kD)^2}{(kD - z_i)^2 + z_r^2} \quad (25)$$

Thus if z_i is decreased by the noninternal impedance portion of Eq. 24, this can be compensated for, to order kD , by decreasing kD by a similar amount. In other words

$$\delta(kD) = -\frac{kd}{2\pi} \left[\ell n \left(\frac{d}{2\pi a} \right) + \sum_{n=1}^{\infty} \left(\frac{1}{\sqrt{n^2 - (d/\lambda)^2}} - \frac{1}{n} \right) - \sum_{n=1}^{\infty} \frac{e^{-\frac{4\pi D}{d} \sqrt{n^2 - (d/\lambda)^2}}}{\sqrt{n^2 - (d/\lambda)^2}} \right] \quad (26)$$

or, since we are in the region where (d/λ) is small,

$$\delta(kD) = -\frac{kd}{2\pi} \left[\ell n \left(\frac{d}{2\pi a} \right) - \sum_{n=1}^{\infty} \frac{e^{-4\pi n(D/d)}}{n} \right] \quad (27)$$

i. e.

$$\frac{\delta D}{d} = -\frac{1}{2\pi} \ell n \left[\frac{d}{2\pi a} \left(1 - e^{-4\pi(D/d)} \right) \right]. \quad (28)$$

If D is greater, or of the same size, as d , the above equation reduces quite accurately to

$$\frac{\delta D}{d} = -\frac{1}{2\pi} \ell n \left(\frac{d}{2\pi a} \right). \quad (29)$$

Equation 29 is the same as that derived from static considerations in Ref. [5], for the case of an isolated set of wires in space (note that the "d" of Ref. [5], Eq. 88, is twice the "d" of the present note, and that the wire radius is denoted by "c" in Ref. [5]). The conditions for the validity of Eq. 28 are that both d/λ and D/λ be small. The further condition for the validity of Eq. 29 is that D be of the same order as d , or larger.

An objection to the above method of compensating for wire discreteness is the necessity that kD be very small. For such frequencies there can be very little energy absorption, as can be seen from Eqs. 15 and 25. The distance adjustment mostly just corrects the phase of the reflected wave to that predicted by a uniform sheet analysis.

Perhaps a better way to go from a uniform sheet to a set of wires is to accept the fact that the wires inevitably represent an inductance at low frequency. The result of this acceptance is that we can use uniform sheet designs by requiring only d/λ to be small, D/λ being unrestricted. We design a uniform sheet and then load the wires by the required inductance per unit length minus the unavoidable inductance. From Eq. 24, the unavoidable inductance per unit length is given, for small d/λ , by

$$L_o = \frac{\mu_o}{2\pi} \lambda n \left\{ \frac{d}{2\pi a} \left(1 - e^{-4\pi D/d} \right) \right\} . \quad (30)$$

This inductance can be made quite small by choosing appropriate values of "d" and "a", or it can be allowed for in the uniform sheet design. The condition for the validity of Eq. 30 is that d/λ be small.

II. E Resistive Sheets for Minimum Average Reflection

If resistive sheets can be fabricated as a set of resistive wires by some method such as making sure d/λ is small, they are just about the easiest reflection reducer to construct. For this reason it behooves us to find out just what can be done with resistive sheets.

One criterion for a resistive sheet could be that it minimizes the average reflected energy over a broad frequency band. Let us see what value of z_r (assumed to be frequency-independent) accomplishes this. If z_i is zero, Eq. 14 reduces to

$$|R|^2 = \frac{z_r^2 + \sin^2 kD (1 - 2z_r)}{z_r^2 + \sin^2 kD (1 + 2z_r)} \quad (31)$$

The right hand side of this equation is periodic in (kD) . Integrating it with respect to (kD) from zero to 2π and dividing by 2π , we obtain

$$\langle |R|^2 \rangle = \frac{2z_r^2 - z_r + 1}{2z_r^2 + 3z_r + 1} \quad (32)$$

The value of z_r for which this expression attains its minimum is given by

$$z_r = 1/\sqrt{2} \quad (33)$$

at which point

$$\begin{aligned} \langle |R|^2 \rangle_{\min} &= \frac{2\sqrt{2} - 1}{2\sqrt{2} + 3} \\ &= .3137 \end{aligned} \quad (34)$$

II. F Resistive Sheets for Minimum Reflection at a Given Frequency

Another possible way of designing a resistive sheet is to minimize the reflected energy for a particular chosen value of kD (this might correspond roughly to some external resonant frequency of the system under test). It is a simple matter to find the minimum of the right hand side of Eq. 31 for some fixed kD ($\equiv k_0 D$). This minimum occurs when

$$z_r = \sin k_0 D \quad (35)$$

and is given by

$$|R|_{\min}^2 = \frac{1 - \sin k_0 D}{1 + \sin k_0 D} \quad (36)$$

II. G Optimum Resistive Sheets for Particular Pulses

In Sec. II. E we discussed minimizing the average reflected energy over a broad frequency band. This is equivalent to minimizing the reflected energy for very short, or delta-function, incident pulses. A more general way to minimize the reflected energy if something more definite is known about the incident pulse comes readily to mind. One merely minimizes the integral of Eq. 31 multiplied by the energy spectrum of the incident pulse by an appropriate choice of z_r (keeping the incident energy constant).

For example, suppose our incident pulse is given by $U(t)e^{-t/\tau}$, where $U(t)$ is a unit step function. The Fourier transform of this pulse is just $(i\omega - 1/\tau)^{-1}$, and thus the incident energy spectrum is proportional to $(\tau^{-2} + \omega^2)^{-1}$, i. e. to $(X_0^2 + (kD)^2)^{-1}$, where $X_0 = (D/\tau c)$. Thus we must minimize the ratio of integrals

$$f = \frac{\int_0^\infty \frac{z_r^2 + \sin^2 X(1 - 2z_r)}{z_r^2 + \sin^2 X(1 + 2z_r)} \cdot \frac{dX}{X_0^2 + X^2}}{\int_0^\infty \frac{dX}{X_0^2 + X^2}} \quad (37)$$

The integral in the denominator of Eq. 37 is trivial, while the one in the numerator can be split into one that is the same as the denominator and a tabulated integral ([6], p. 440, No. 3.813.2). The result, after algebraic simplification is that

$$f = 1 - \frac{4z_r T}{z_r^2(T + 1) + 3z_r T + T} \quad (38)$$

where

$$T \equiv \tanh X_0. \quad (39)$$

Minimizing f with respect to z_r we find that the appropriate value of z_r is given by

$$z_r = \sqrt{\frac{T}{1+T}} = \sqrt{\frac{1 - e^{-2X_0}}{2}} \quad (40)$$

and that the minimum f is given by

$$\begin{aligned} f_{\min} &= \frac{2 - \sqrt{\frac{T}{1+T}}}{2 + 3\sqrt{\frac{T}{1+T}}} \\ &= \frac{2\sqrt{2} - \sqrt{1 - e^{-2X_0}}}{2\sqrt{2} + 3\sqrt{1 - e^{-2X_0}}} \end{aligned} \quad (41)$$

By numerical evaluation it can be shown that f_{\min} is less than .5 as long as X_0 ($\equiv D/\tau c$) is greater than .089.

II. H Resistive Sheets at Low Frequency

Reflection reducing sheets can not help much at very low frequency. The reflection coefficients of any finite number of resistive sheets in front of a perfectly conducting plane must approach unity as the frequency approaches zero. Nevertheless, because the expected incident pulse has a significant low energy content, one should try to bring the reflection coefficient down from unity as rapidly as possible with increasing frequency. A way to partially achieve this with resistive sheets can be seen from the low frequency expansion of Eq. (31), which is

$$|R|^2 \rightarrow 1 - \frac{4(kD)^2}{z_r} \quad (42)$$

Thus a low value of z_r will increase the initial quadratic drop-off of $|R|^2$ with w . Unfortunately this is paid for by raising the value to which $|R|^2$ eventually drops. This kind of minimum for $|R|^2$ is given by

$$|R|_{\min}^2 = \left(\frac{1 - z_r}{1 + z_r} \right)^2 \quad (43)$$

From this we see that, if we restrict ourselves to resistive sheets, we can have either a fast drop-off to a fairly high value of $|R|^2$ or a fairly slow drop-off to a very low value of $|R|^2$, and thus some compromise must be made. Another kind of price one can pay for a fast initial drop-off is discussed in Sec. II. J.

II. I Inductive-Resistive Null-Design Sheets

Another possible way of designing impedance sheets is to create a complete null in the reflection coefficient for some particular frequency for which, for any reason, we expect a great deal of the incident energy to be concentrated. This can be accomplished by inductive-resistive sheets (to be fabricated by inserting series inductive elements in resistive wires) if the critical values of kD is between $\pi/2$ and π .

To determine the appropriate sheet impedance let us see what values of z_r and z_i will make the α of Eq. 16 equal to unity for $k = k_0$. For these values of α and k , Eq. 16 can be rewritten as

$$\sin^2 k_0 D + z_r^2 + z_i^2 - 2z_i \sin k_0 D \cos k_0 D - 2z_r \sin^2 k_0 D = 0 \quad (44)$$

or, rearranging the terms, as

$$(z_r - \sin^2 k_o D)^2 + (z_i - \sin k_o D \cos k_o D)^2 = 0 \quad (45)$$

Both terms of the above equation are non-negative. Therefore, for a complete null at k_o we must necessarily have

$$\begin{aligned} z_r &= \sin^2 k_o D \\ z_i &= \sin k_o D \cos k_o D \end{aligned} \quad (46)$$

We have chosen a time variation of $e^{-i\omega t}$, making the reactance of an inductance negative. For z_i to be negative (and for $k_o D$ to be less than π , which is the most probable place for a null to be necessary) we must have $\pi/2 \leq k_o D \leq \pi$. Assuming a series resistance and inductance per unit length in the grid wires, of values R_w and L_w , we have from Eqs. 23, 24 and 46 (for the small d/λ implicit in the sheet assumption),

$$\begin{aligned} R_w &= (Z_o/d) \sin^2 k_o D \\ L_w &= (Z_o/d) (\sin k_o D \cos k_o D / \omega_o) \end{aligned} \quad (47)$$

Using these values of R_w and L_w , the equation for α can be written as

$$\begin{aligned} \alpha &= (Z \sin^2 kD \sin^2 k_o D) / (\sin^2 kD + \sin^4 k_o D + \left(\frac{\omega}{\omega_o}\right)^2 \sin^2 k_o D \cos^2 k_o D \\ &\quad - \frac{2\omega}{\omega_o} \sin k_o D \cos k_o D \sin kD \cos kD) \end{aligned} \quad (48)$$

from which $|R|^2$ can be written as

$$\begin{aligned} |R|^2 &= \frac{1 - \alpha}{1 + \alpha} \\ |R|^2 &= \frac{\left(\sin^2 kD - \sin^2 k_o D\right)^2 + \left(\frac{\omega}{\omega_o} \sin k_o D \cos k_o D - \sin kD \cos kD\right)^2}{\left(\sin^2 kD + \sin^2 k_o D\right)^2 + \left(\frac{\omega}{\omega_o} \sin k_o D \cos k_o D - \sin kD \cos kD\right)^2} \end{aligned} \quad (49)$$

This equation for $|R|^2$ is plotted versus D/λ in Fig. 4 for several values of D/λ_0 (note that $D/\lambda = kD/2\pi$). The most striking thing about Fig. 4 is that the more we shove D/λ_0 toward $\frac{1}{2}$, the sharper and deeper the null becomes. The simple resistive sheet has a natural null when D/λ_0 is $\frac{1}{4}$. The more we try to avoid this natural null position by reactive loading the less effective the sheet is in a broad-band sense. Nevertheless, the present analysis indicates a quick way of adjusting for unpredicted peaks in the incident radiation once the grid structure is in place. This is especially true since the exact value of R_w is not too critical. This can be seen from Fig. 5, where the value of L_w is chosen according to Eq. 24, but the value of R_w is always set at (Z_0/d) . It can be seen that the "nulls" thus created are not precisely zero, but that the approximate null can be shifted somewhat (although rather sluggishly) by varying L_w alone. This method has the added benefit that the shifted "nulls" are still fairly broad.

II. J Capacitive-Resistive Null-Design Sheets

To create a null for $k_0 D$ less than $\pi/2$, a sheet made up of resistive elements in parallel with capacitive elements is one possibility. This is so because, rewriting the equation for α in terms of sheet admittance, we have

$$\alpha = \frac{2 \sin^2 kD y_r}{1 + |y|^2 \sin^2 kD + 2 y_i \sin kD \cos kD}, \quad (50)$$

and from this, if α is to be unity at k_0 , we must have

$$\sin^2 k_0 D (y_r - 1)^2 + (y_i \sin k_0 D + \cos k_0 D)^2 = 0. \quad (51)$$

The above equation, for a parallel $R_w - C_w$ combination, can only be valid if we set

$$\begin{aligned} y_r &= 1 \\ y_i &= -\cot k_0 D, \end{aligned} \quad (52)$$

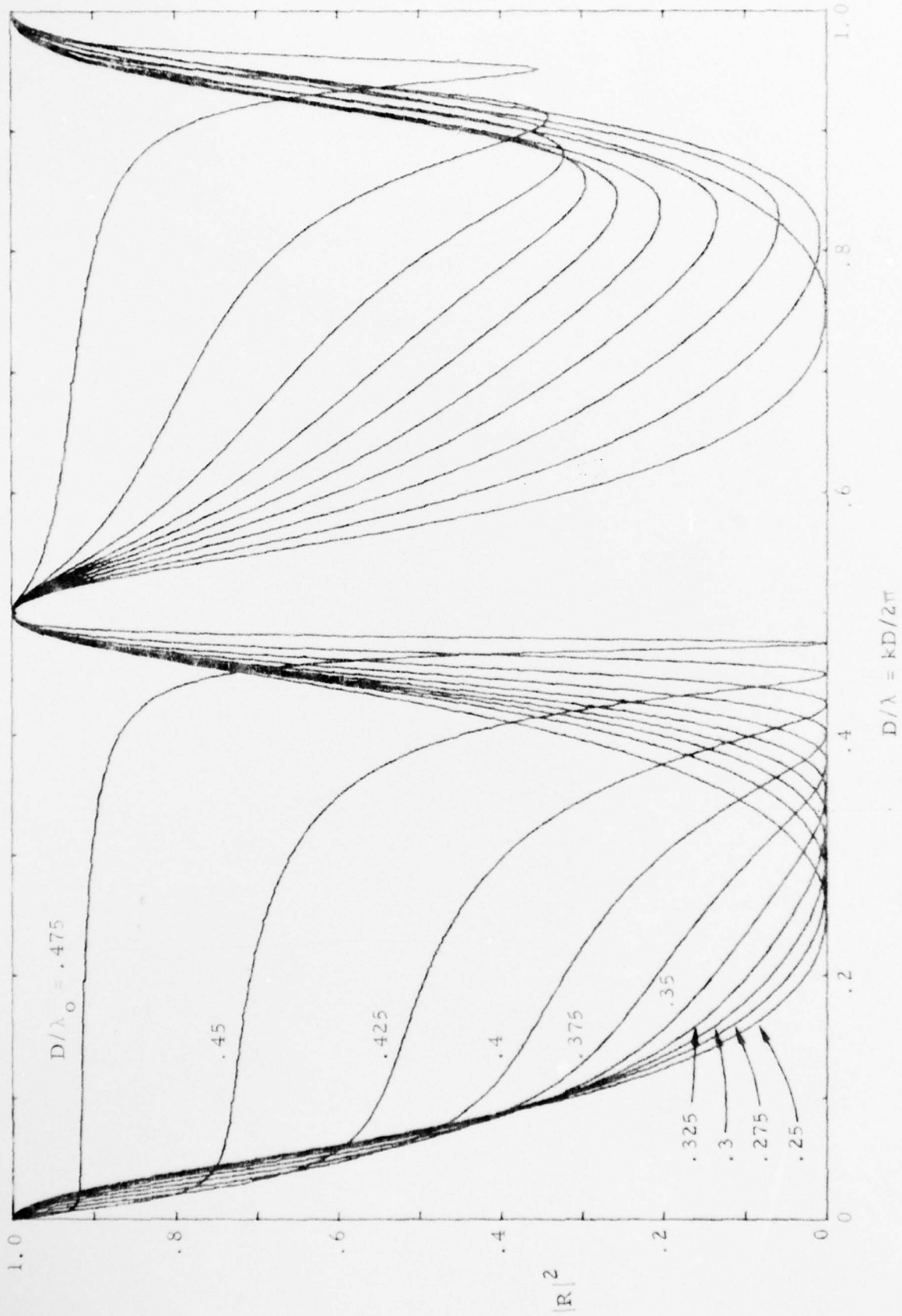


Fig. 4: Inductive-Resistive Null Sheets for Various Values of D/λ_0 ($\equiv k_0 D/2\pi$)

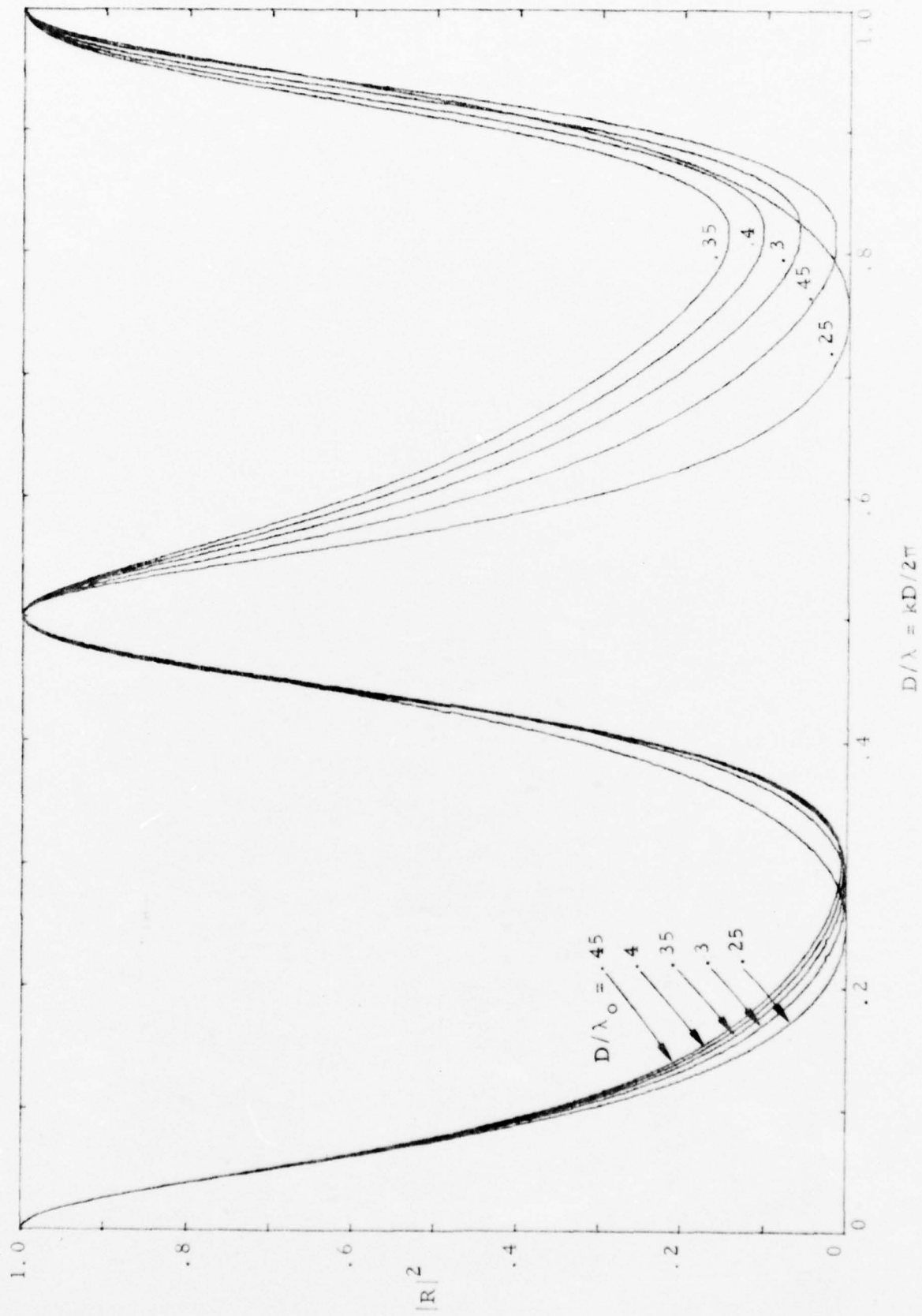


Fig. 5: Approximate Nulls Resulting from Varying L_w Only ($R_w = Z_0/d$)

and thus

$$R_w = Z_o/d$$

$$C_w = (dD\epsilon_o) \frac{\cot k_o D}{k_o D} \quad (53)$$

With these values of R_w and C_w , α can be written as

$$\alpha = (2 \sin^2 kD)/(1 + \sin^2 kD + (w/w_o)^2 \cot^2 k_o D \sin^2 kD$$

$$- 2(w/w_o) \cot k_o D \sin kD \cos kD)$$

$$= (2 \sin^2 kD)/(2 \sin^2 kD + \left(\frac{w}{w_o} \cot k_o D \sin kD - \cos kD\right)^2), \quad (54)$$

from which it follows easily that

$$|R|^2 = \frac{\left(\frac{w}{w_o} \cot k_o D \sin kD - \cos kD\right)^2}{4 \sin^2 kD + \left(\frac{w}{w_o} \cot k_o D \sin kD - \cos kD\right)^2} \quad (55)$$

The plots of Eq. 55 versus D/λ for D/λ less than $\frac{1}{2}$ are almost exactly like the left half of Fig. 4, if we reflect about the $D/\lambda = \frac{1}{4}$ point and set the new D/λ_o equal to $\frac{1}{2}$ minus the D/λ_o of Fig. 4. Thus if we wish to have a null at $D/\lambda_o = .025$, the resulting curve is very similar to the $D/\lambda_o = .475$ curve of Fig. 4, reflected about the $D/\lambda = \frac{1}{4}$ point. Thus we see that we can achieve deep nulls at moderately low frequencies, but that this is paid for in the narrowness of the null (and also in the size of the capacitors necessary, as can be seen from Eq. 53). The width of the null is of the order of $k_o D$.

II. K Explicit Equations for Parameter Study

For the past several subsections we have been discussing impedance sheets, with the implicit assumption that d/λ is small. We now turn to a determination of just what effect d/λ has if it is not so small. This is useful in

judging just what are the limitations of an impedance sheet analysis and also in choosing, from a data presentation, appropriate grid impedances by sight and judgement. This data presentation is given in Sec. III of this note. The explicit equations used in the calculation of this data were

$$|R|^2 = \frac{1 - \alpha}{1 + \alpha}$$

where

$$\alpha = \frac{2z_r \sin^2(2\pi D/\lambda)}{|z_i|^2 + \sin^2(2\pi D/\lambda) - 2z_i \sin(2\pi D/\lambda) \cos(2\pi D/\lambda)}$$

and

$$z_r = R_w d / Z_0$$

$$z_i = - (d/\lambda) \ln(d/2\pi a) - (d/\lambda) \sum_{n=1}^{\infty} \left\{ \frac{1 - e^{-\frac{4\pi D}{d} \sqrt{n^2 - (d/\lambda)^2}}}{\sqrt{n^2 - (d/\lambda)^2}} - \frac{1}{n} \right\}$$

Thus the parameter study is restricted to grids with resistive loading only. The parameters of the study are (d/D) , (d/a) and z_r .

SECTION III

DATA

The following twenty-one sets of curves may be divided into one group of three sets and two groups of nine sets each.

The first group (Figs. 6 through 8) are intended primarily to demonstrate the effect of (d/D) on $|R|^2$. For each of the three, z_r is unity and d/D is the curve-labeling parameter. The three sets are distinguished by different d/a values: 20, 100 and 500.

The next group of nine curve sets (Figs. 9 through 17) is presented to show the effect of z_r on $|R|^2$. The value of z_r is the curve-labeling parameter in each set. The nine sets represent all combinations of three d/a values (20, 100, 500) and three d/D values (1, .5, .1).

The next group of nine curve sets (Figs. 18 through 26) demonstrate the effect of d/a on $|R|^2$ (and, for the left half of these curves, the effect of d/a is quite accurately that of an equivalent inductance given by Eq. 30). The nine sets represent all combinations of three z_r values (.5, 1, 2) and three d/D values (1, .5, .1).

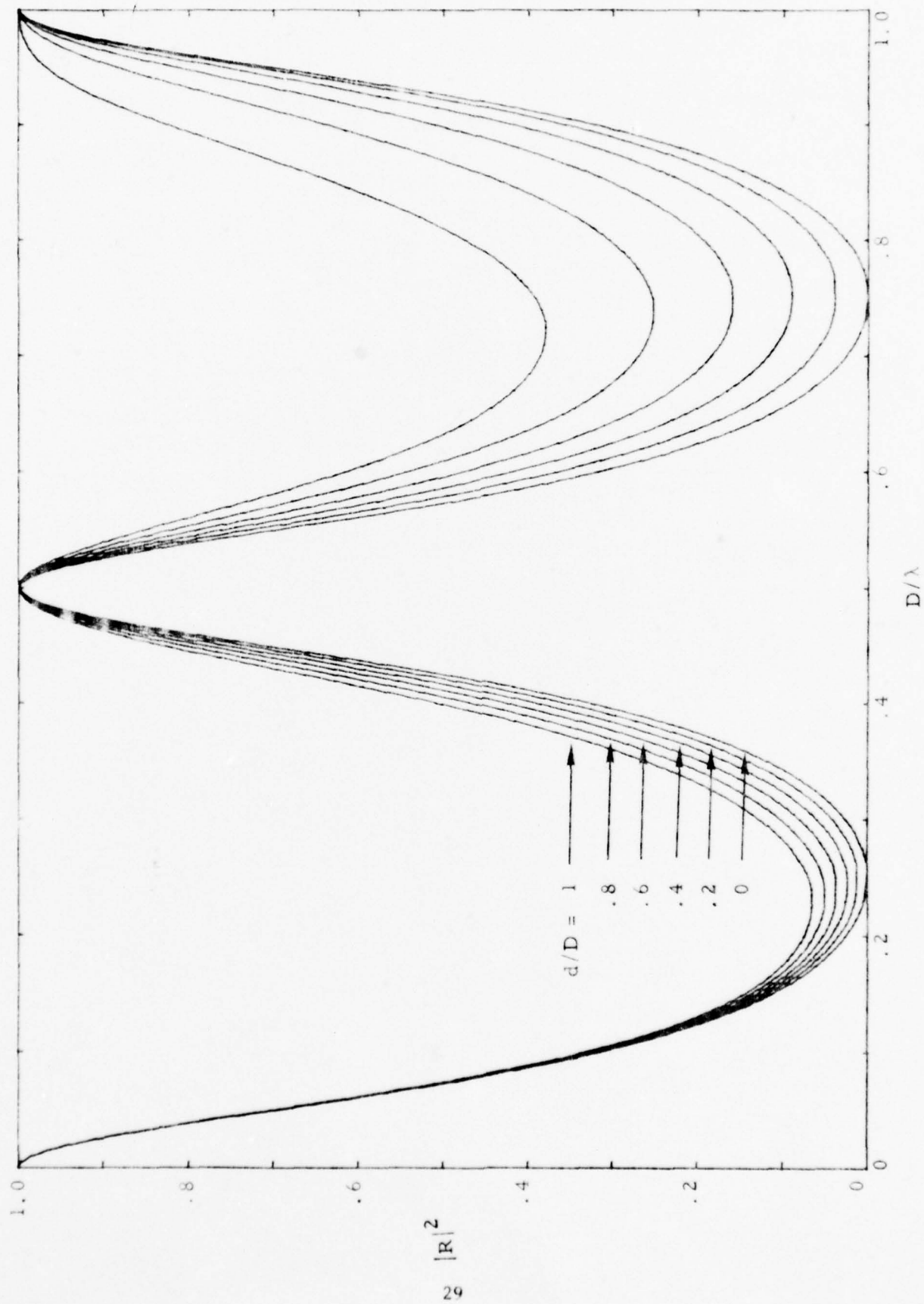


Fig. 6: $|R|^2$ vs. D/λ for $z_r = 1$ and $d/a = 20$

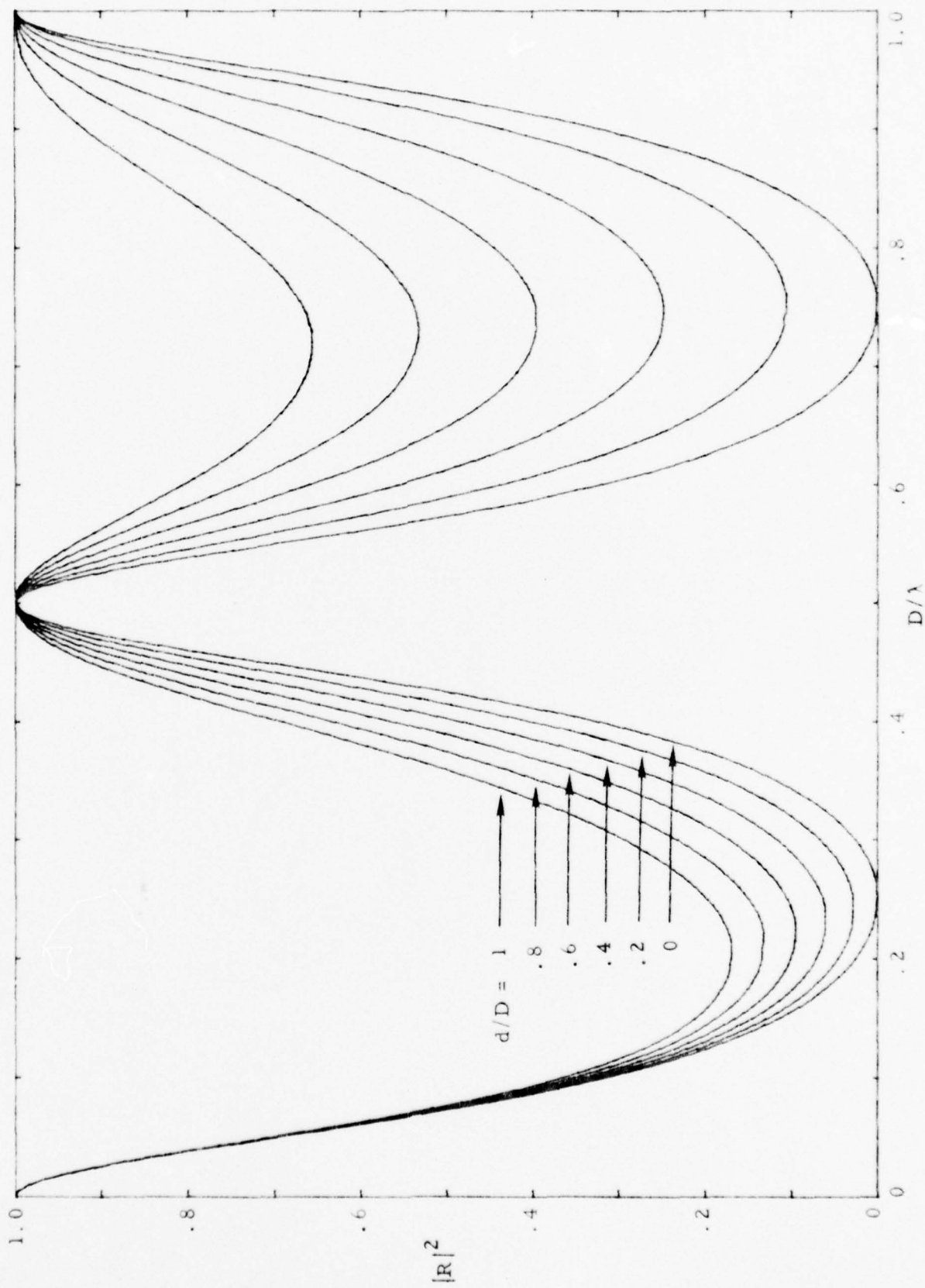


Fig. 7: $|R|^2$ vs. D/λ for $z_r = 1$ and $d/a = 100$

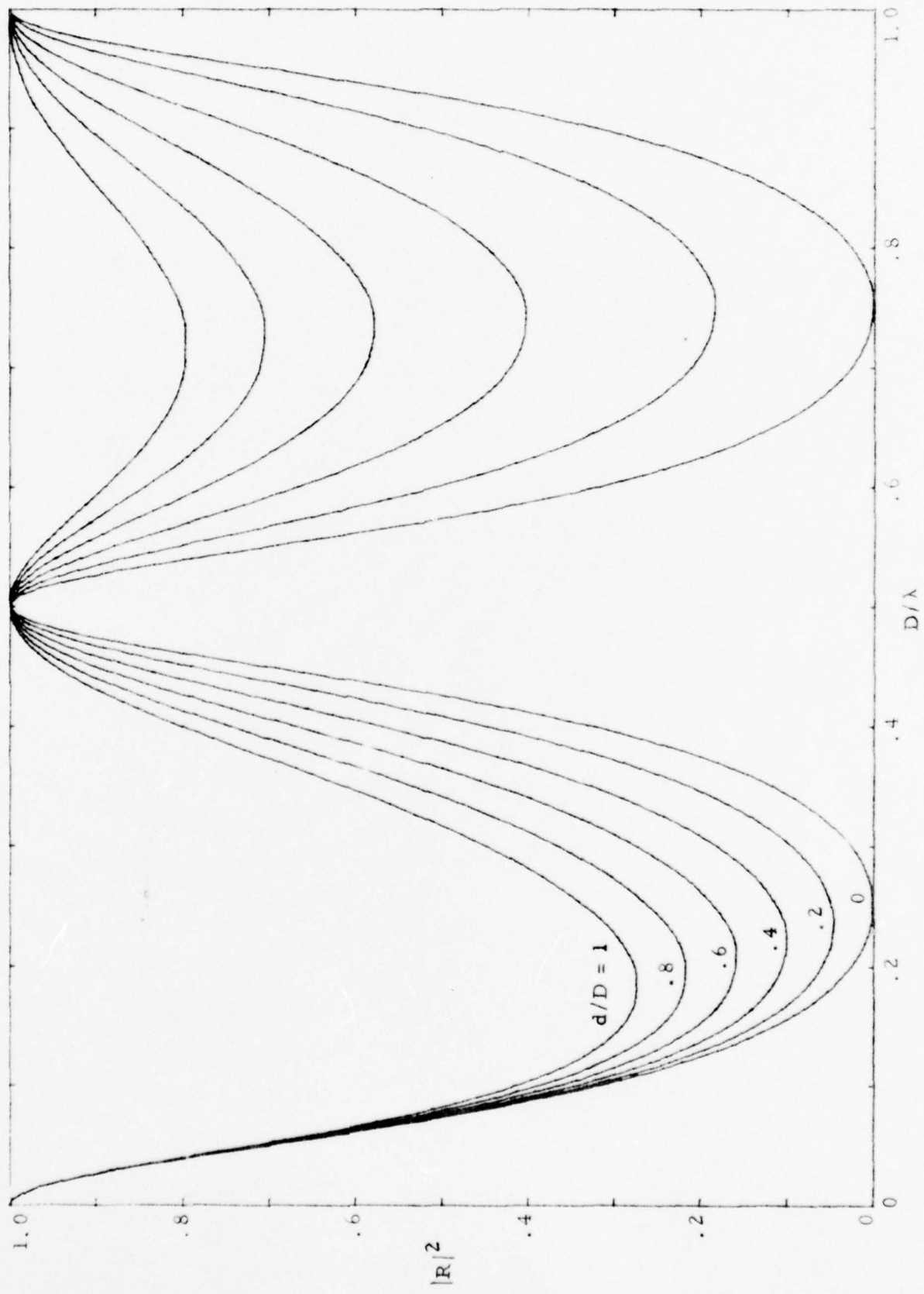


Fig. 8: $|R|^2$ vs. D/λ for $z_T = 1$ and $d/a = 500$

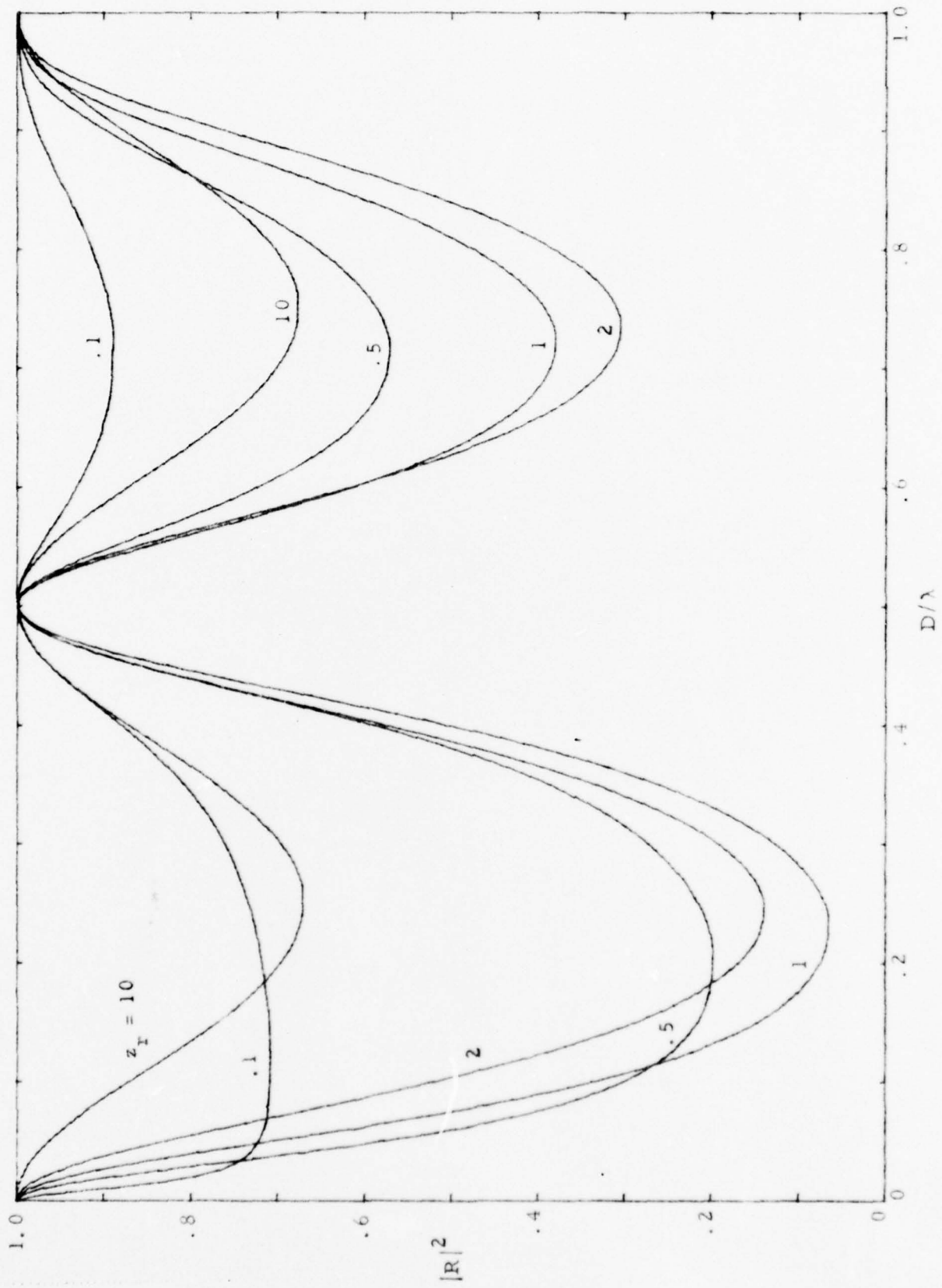


Fig. 9: $|R|^2$ vs. D/λ for $d/a = 20$ and $d/D = 1$

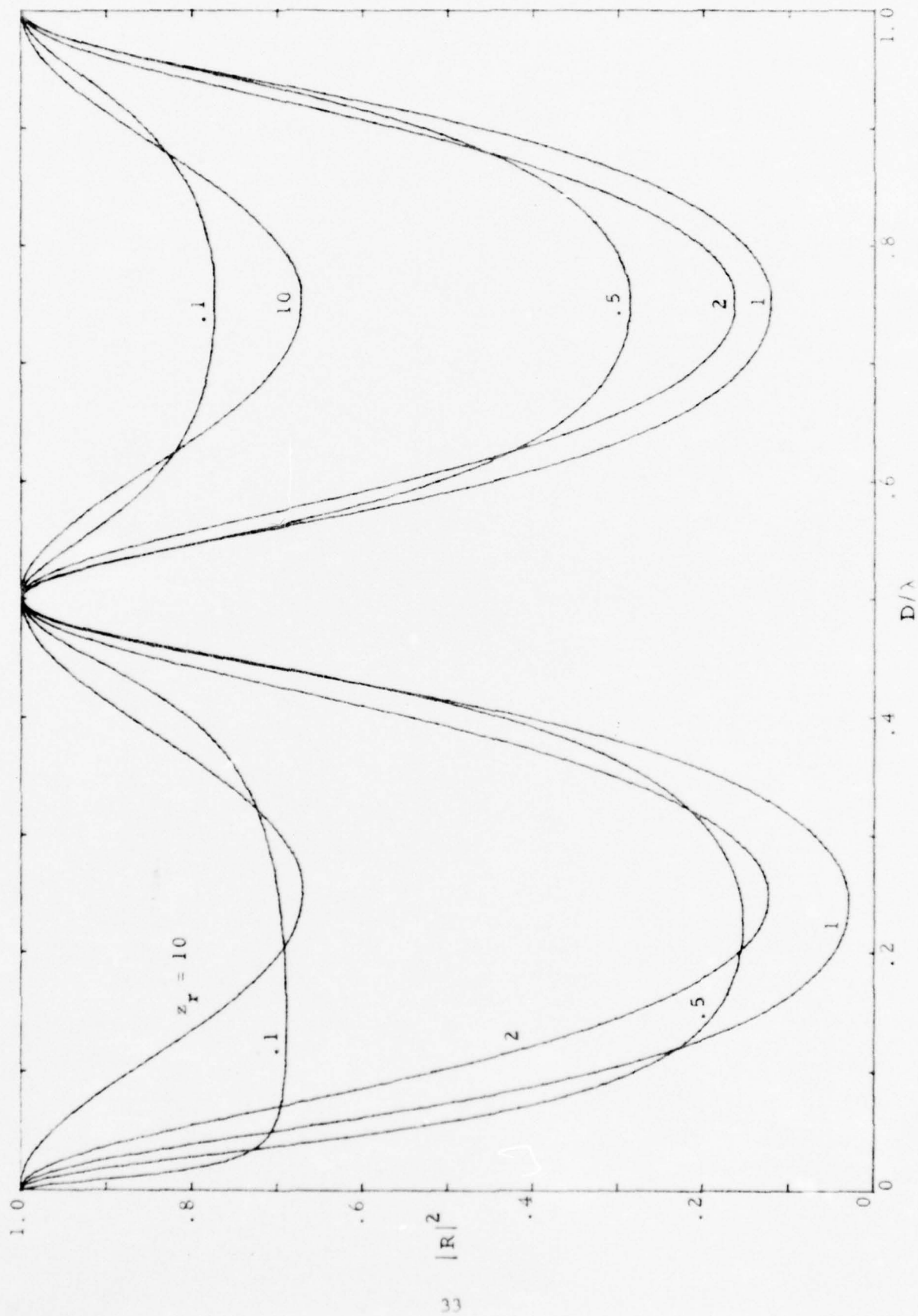


Fig. 10: $|R|^2$ vs. D/λ for $d/a = 20$ and $d/D = .5$

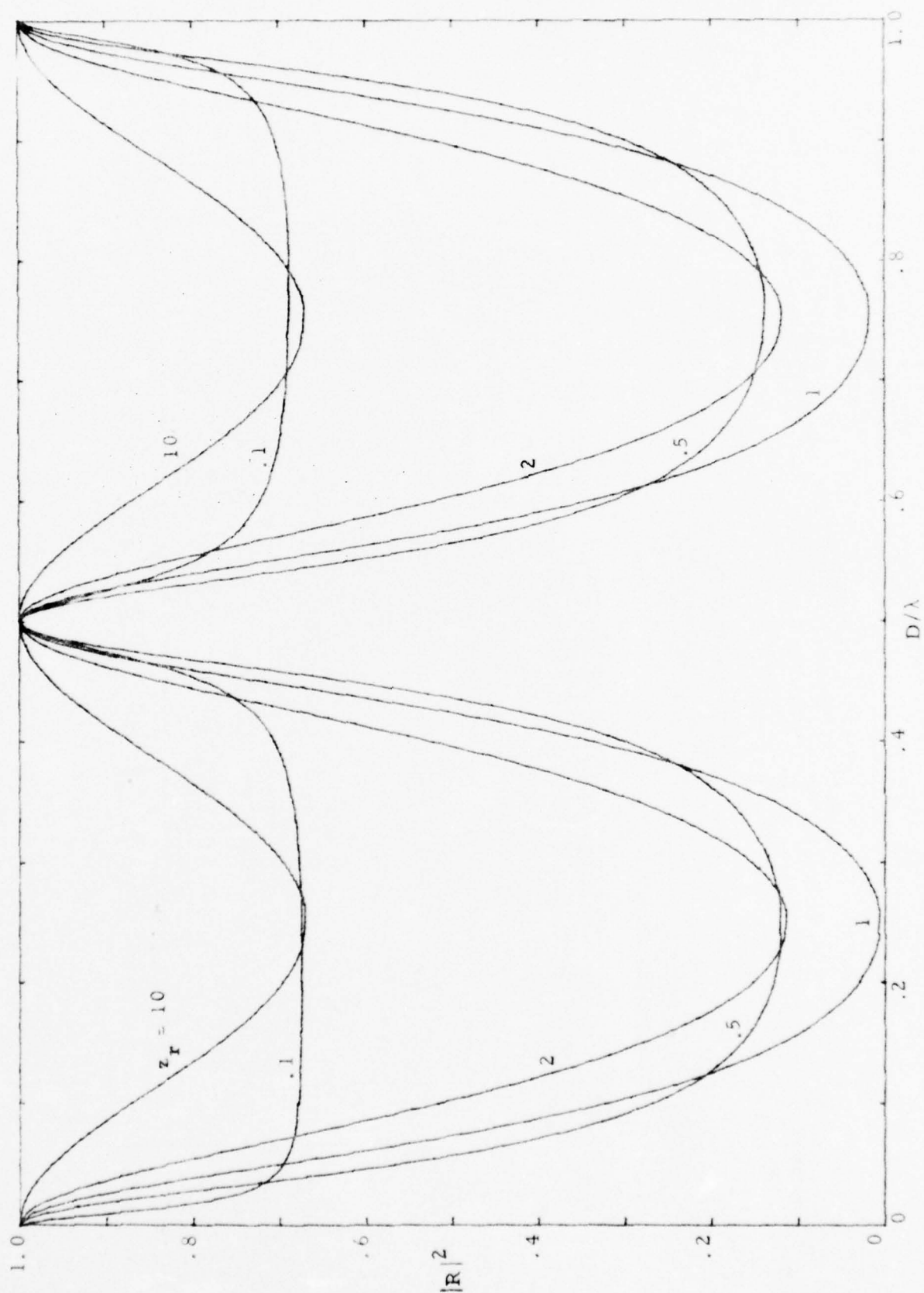


FIG. 11: $|R|^2$ vs. D/λ for $d/a = 20$ and $d/D = .1$

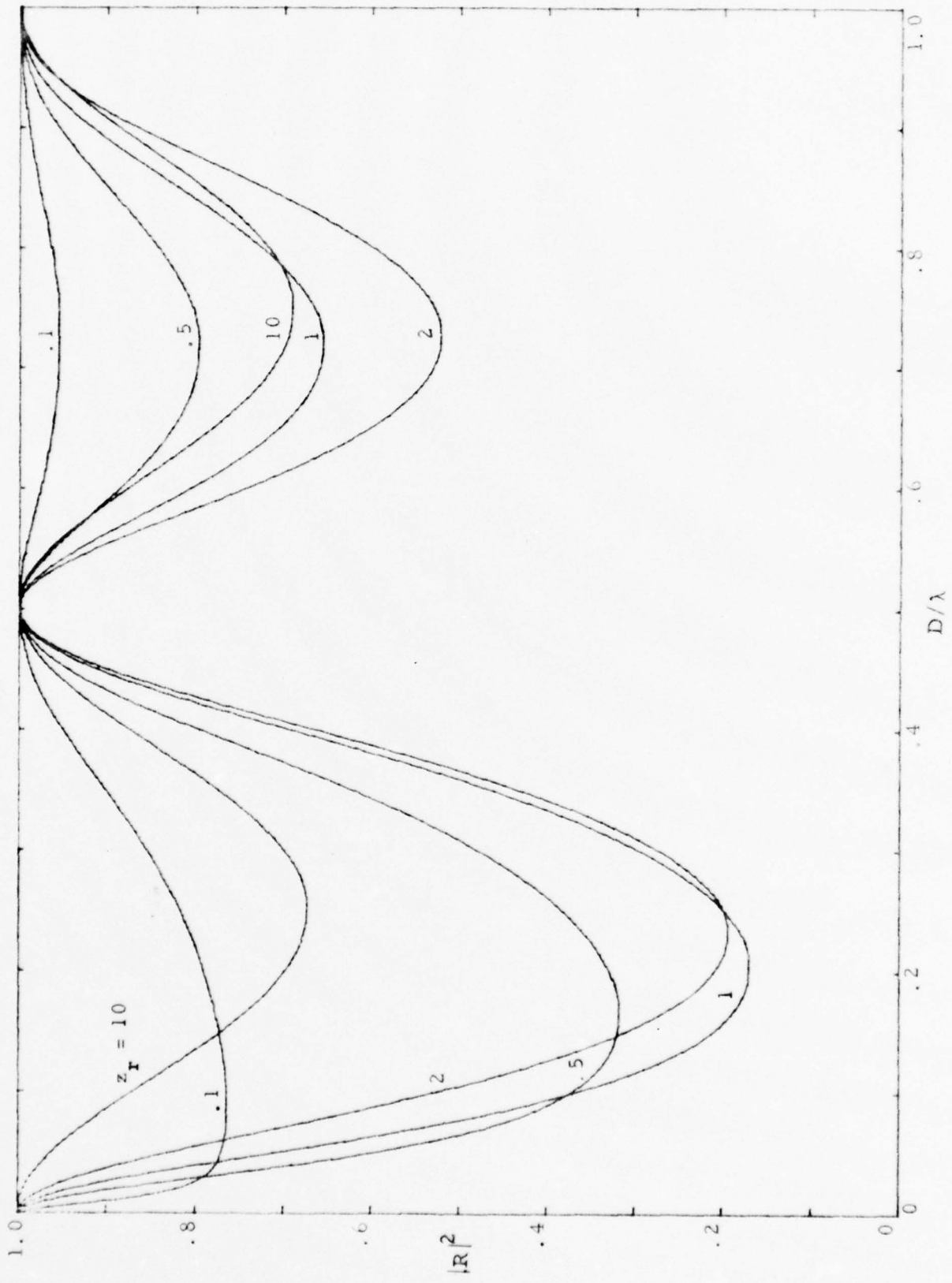


Fig. 12: $|R|^2$ vs. D/λ for $f/a = 100$ and $d/D = 1$

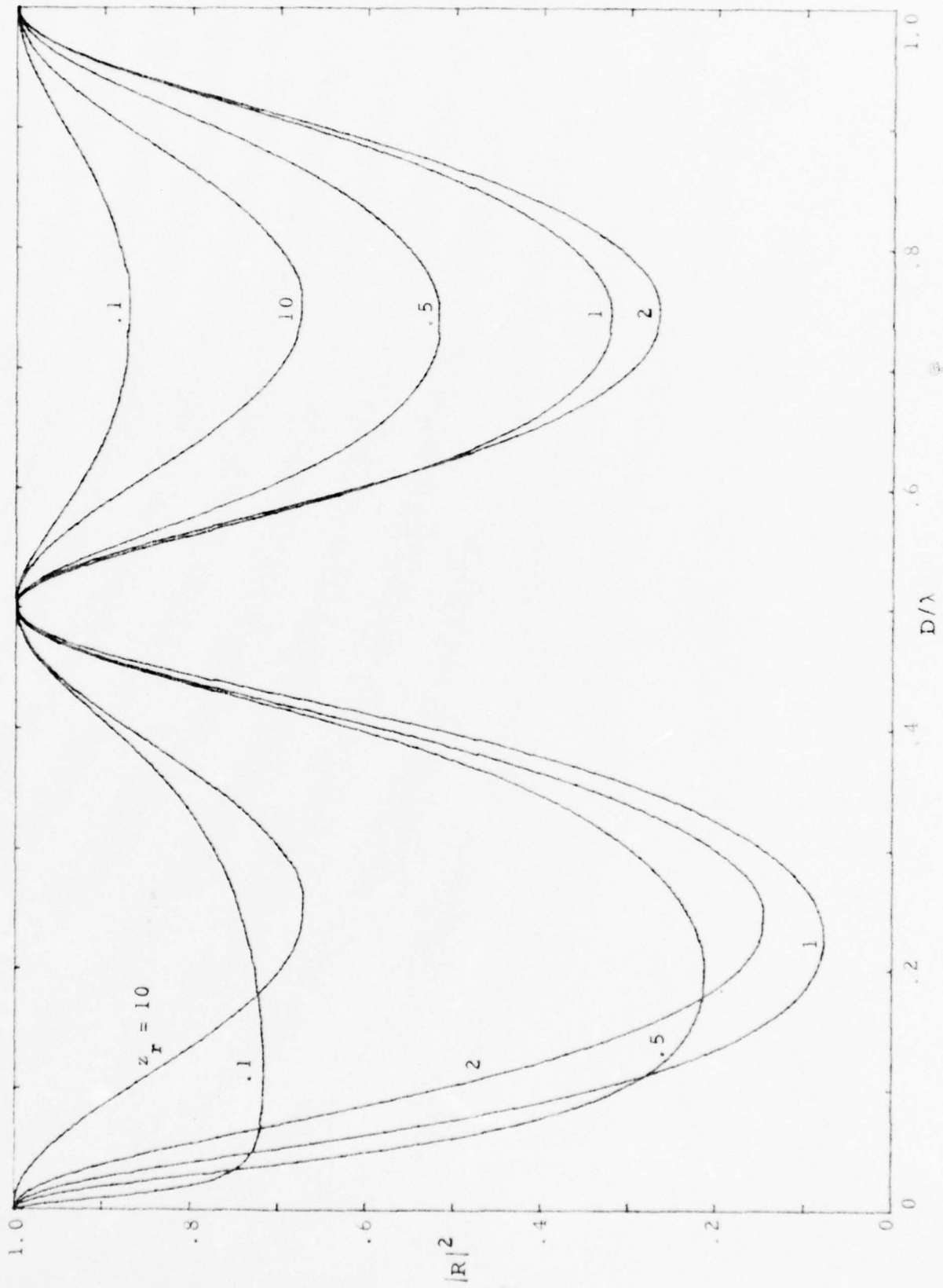


Fig. 13: $|R|^2$ vs. D/λ for $d/a = 100$ and $d/D = .5$

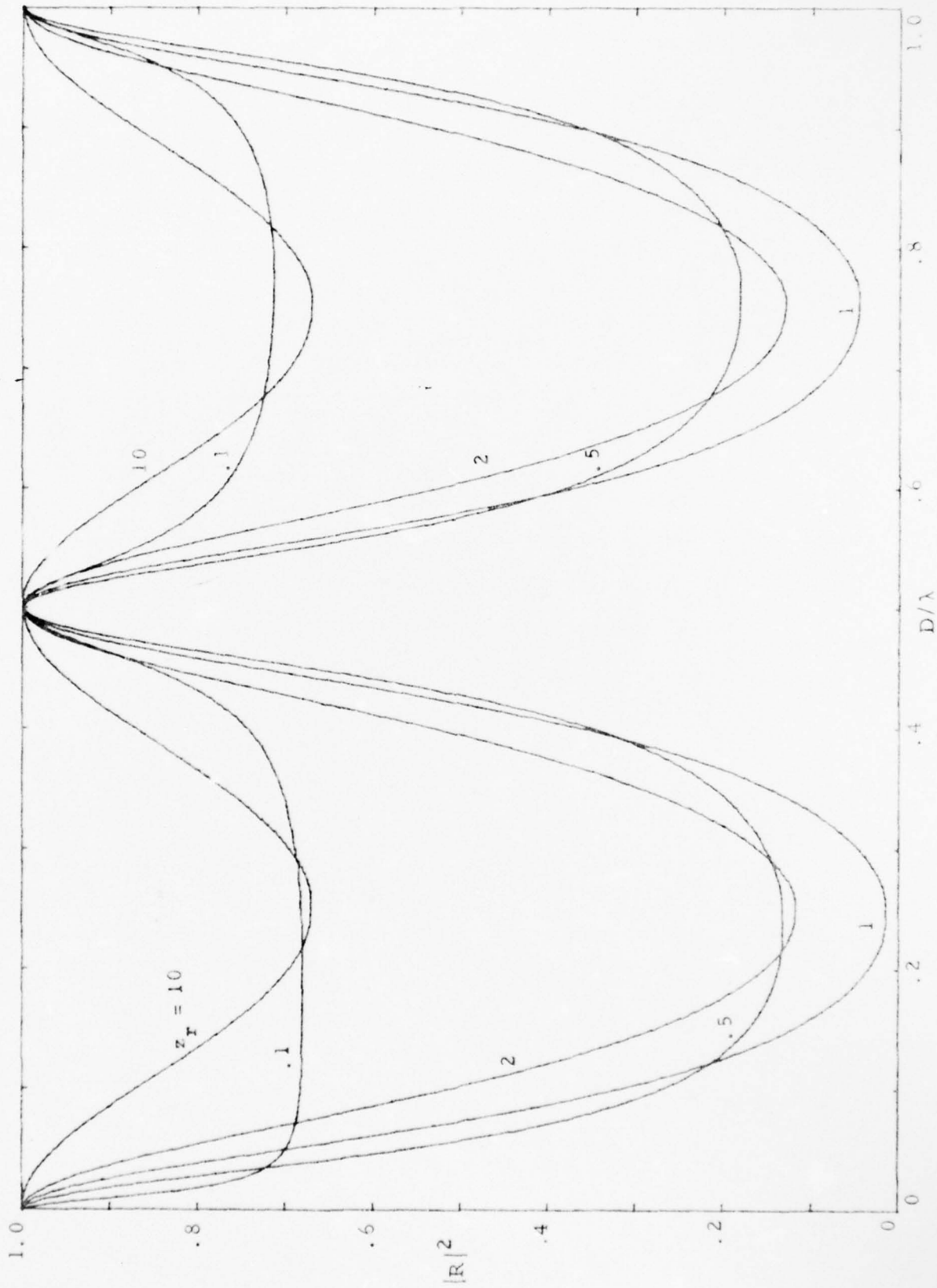


Fig. 14: $|R|^2$ vs. D/λ for $d/a = 100$ and $d/D = .1$

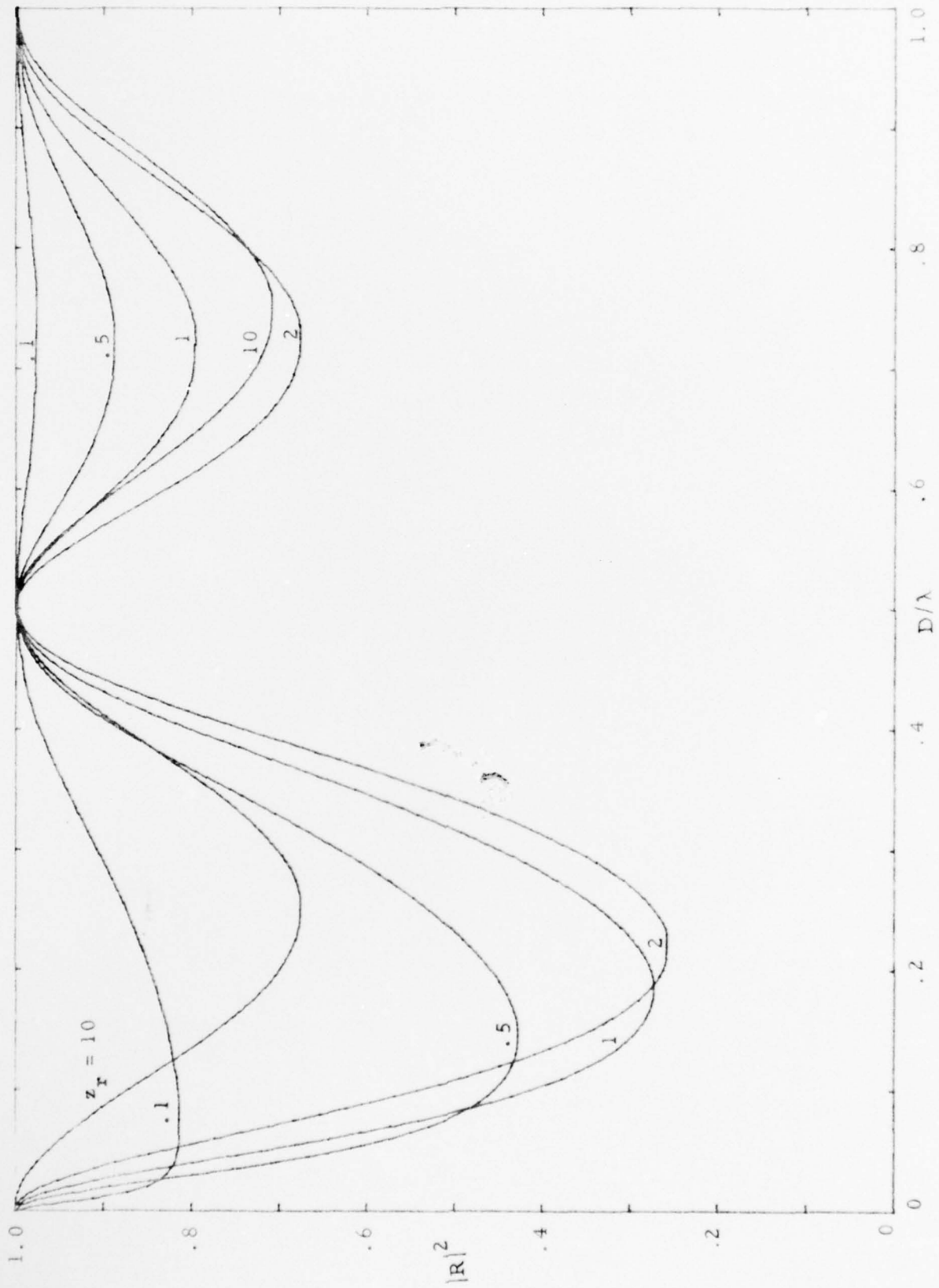


Fig. 15: $|R|^2$ vs. D/λ for $d/a = 500$ and $d/D = 1$

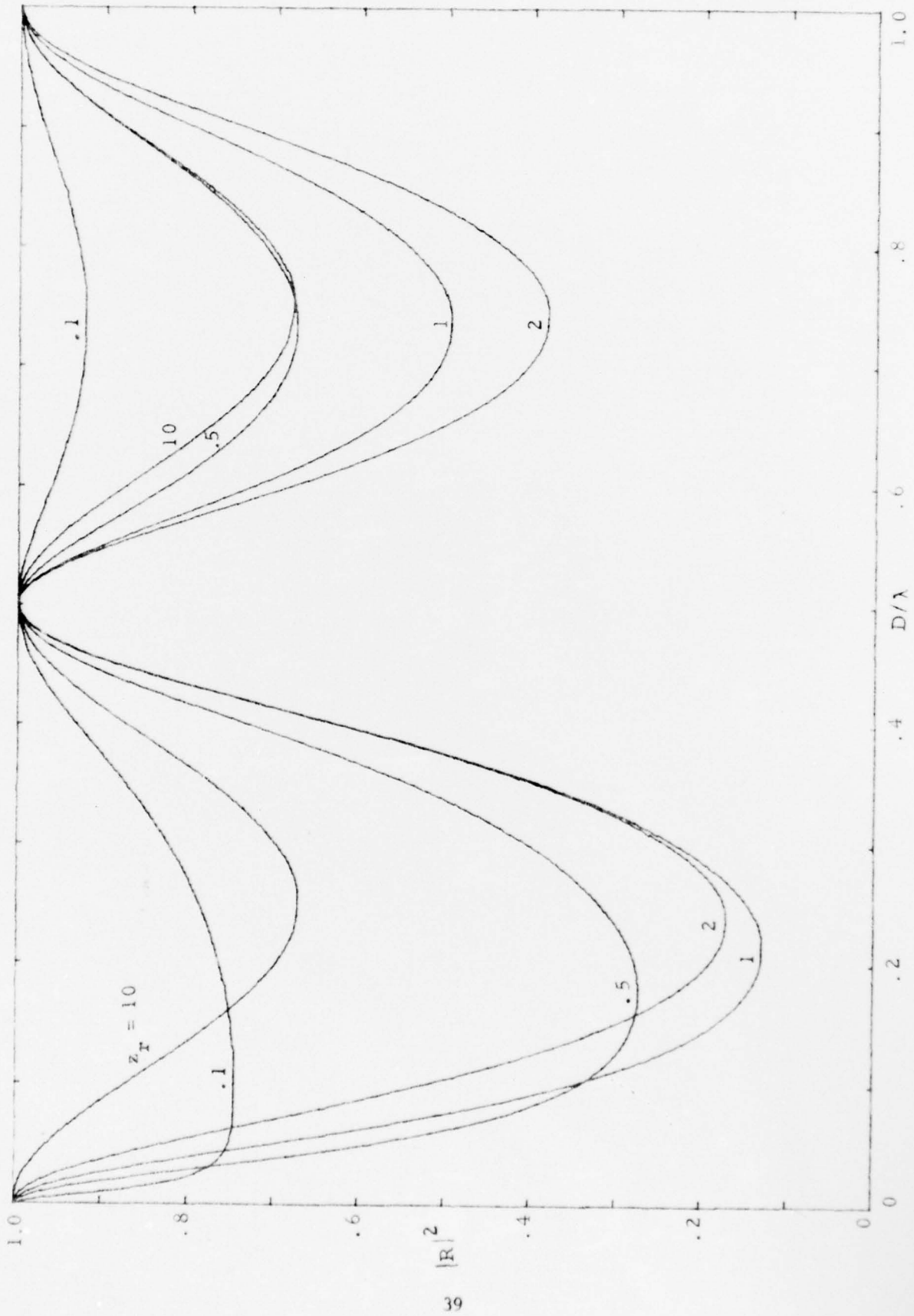


Fig. 16: $|R|^2$ vs. D/λ for $d/a = 500$ and $d/D = .5$

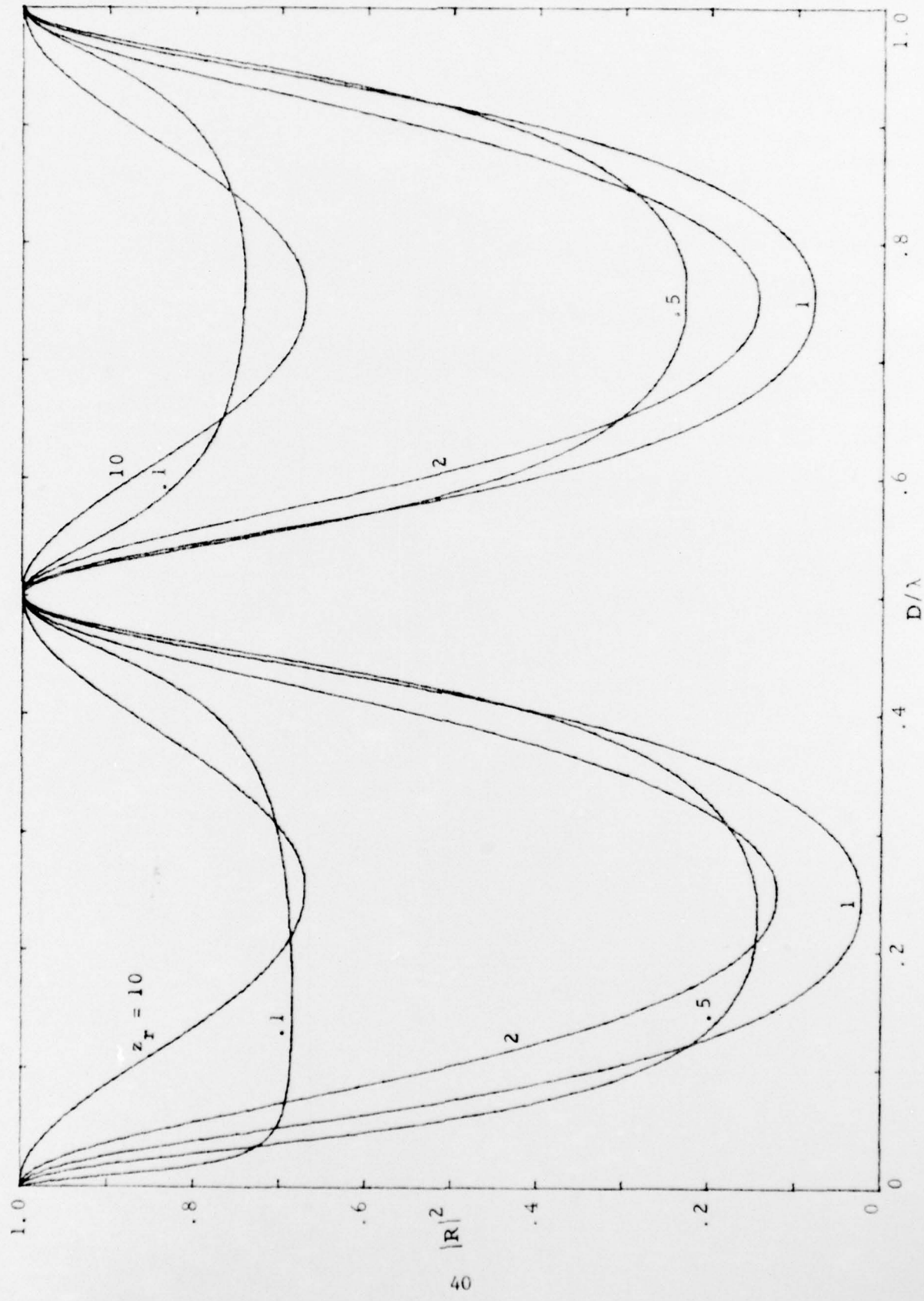


Fig. 17: $|R|^2$ vs. D/λ for $d/a = 500$ and $d/D = .1$

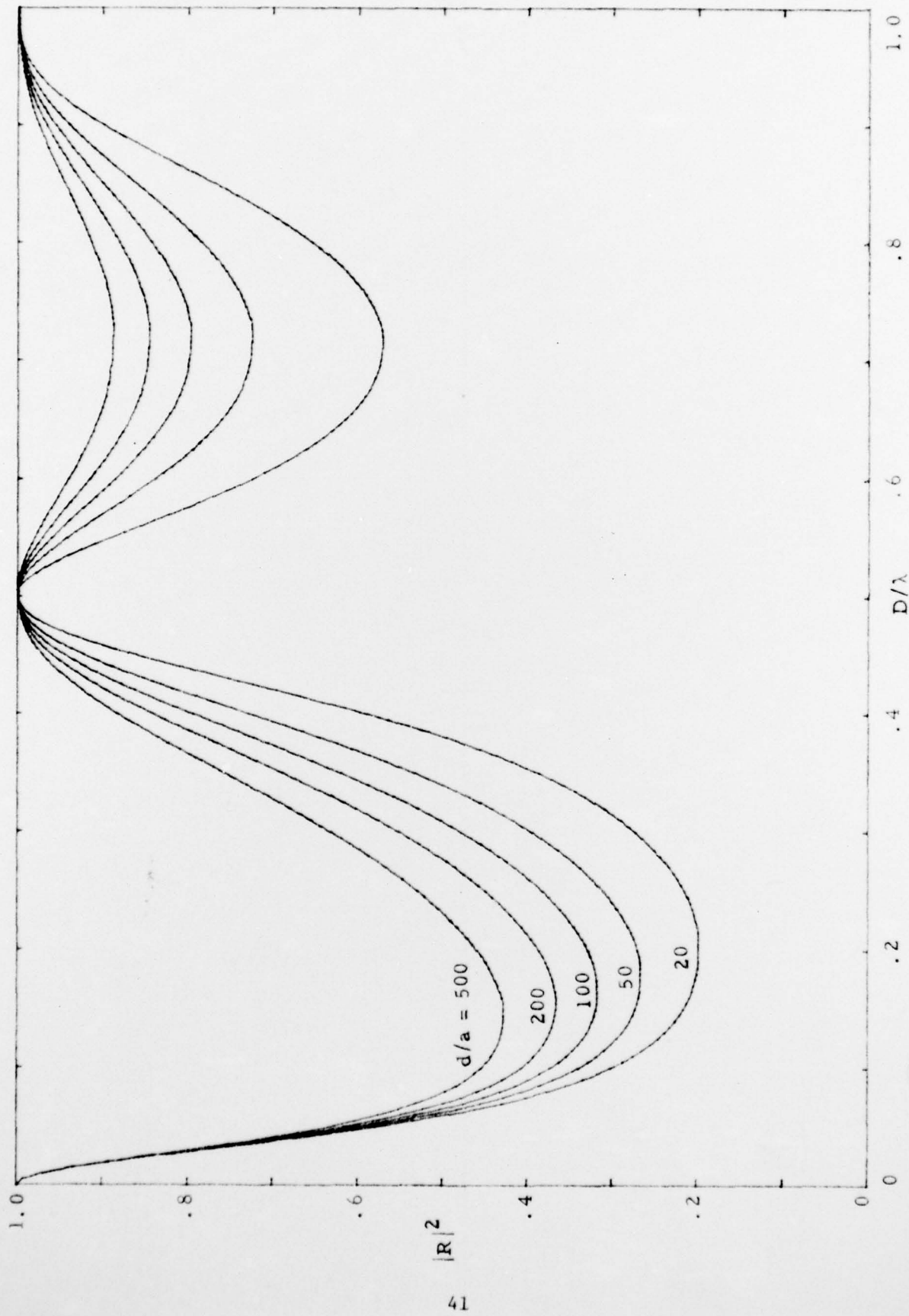


Fig. 18: $|R|^2$ vs. D/λ for $z_r = .5$ and $d/D = 1$

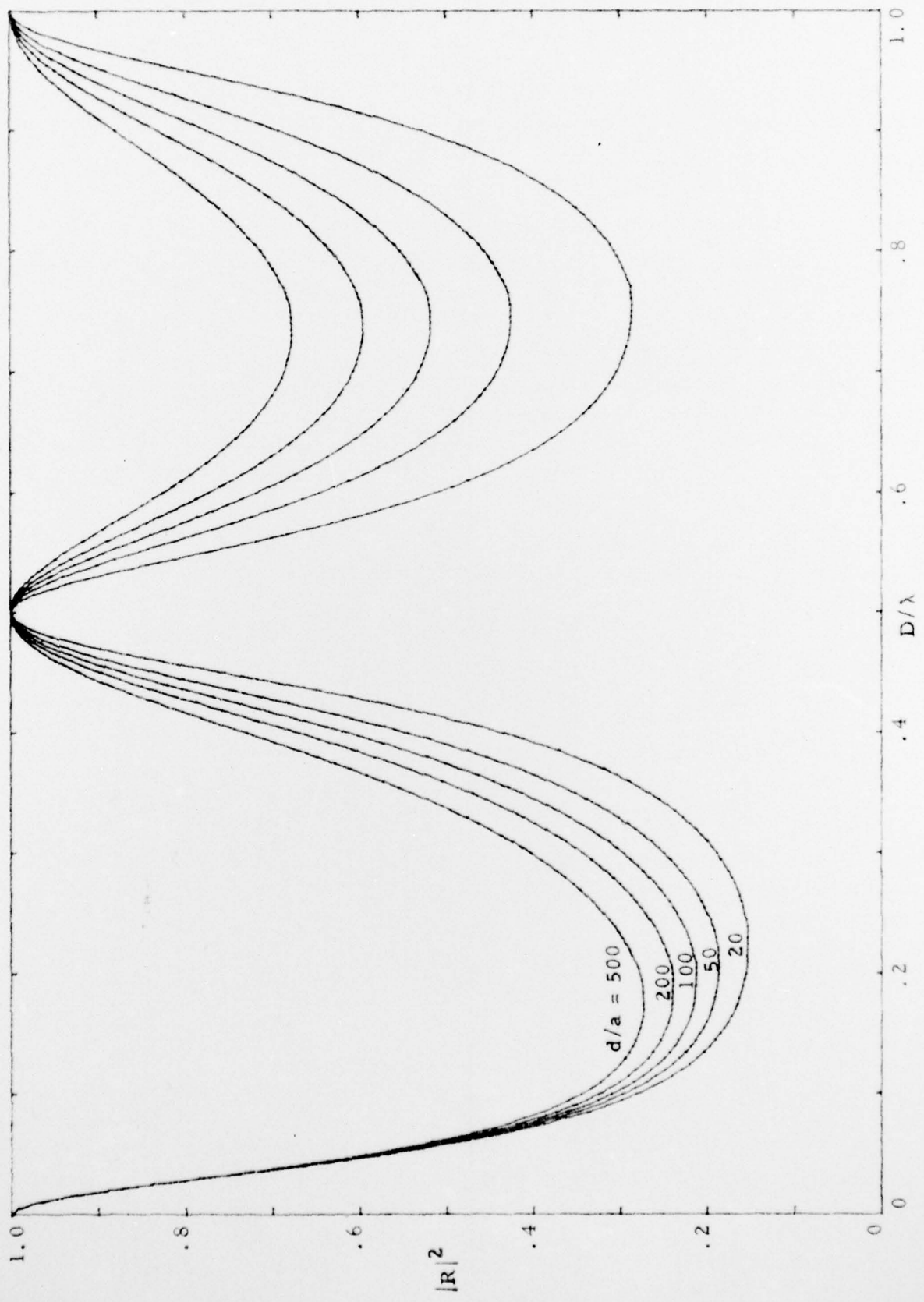


Fig. 19: $|R|^2$ vs. D/λ for $z_r = .5$ and $d/D = .5$

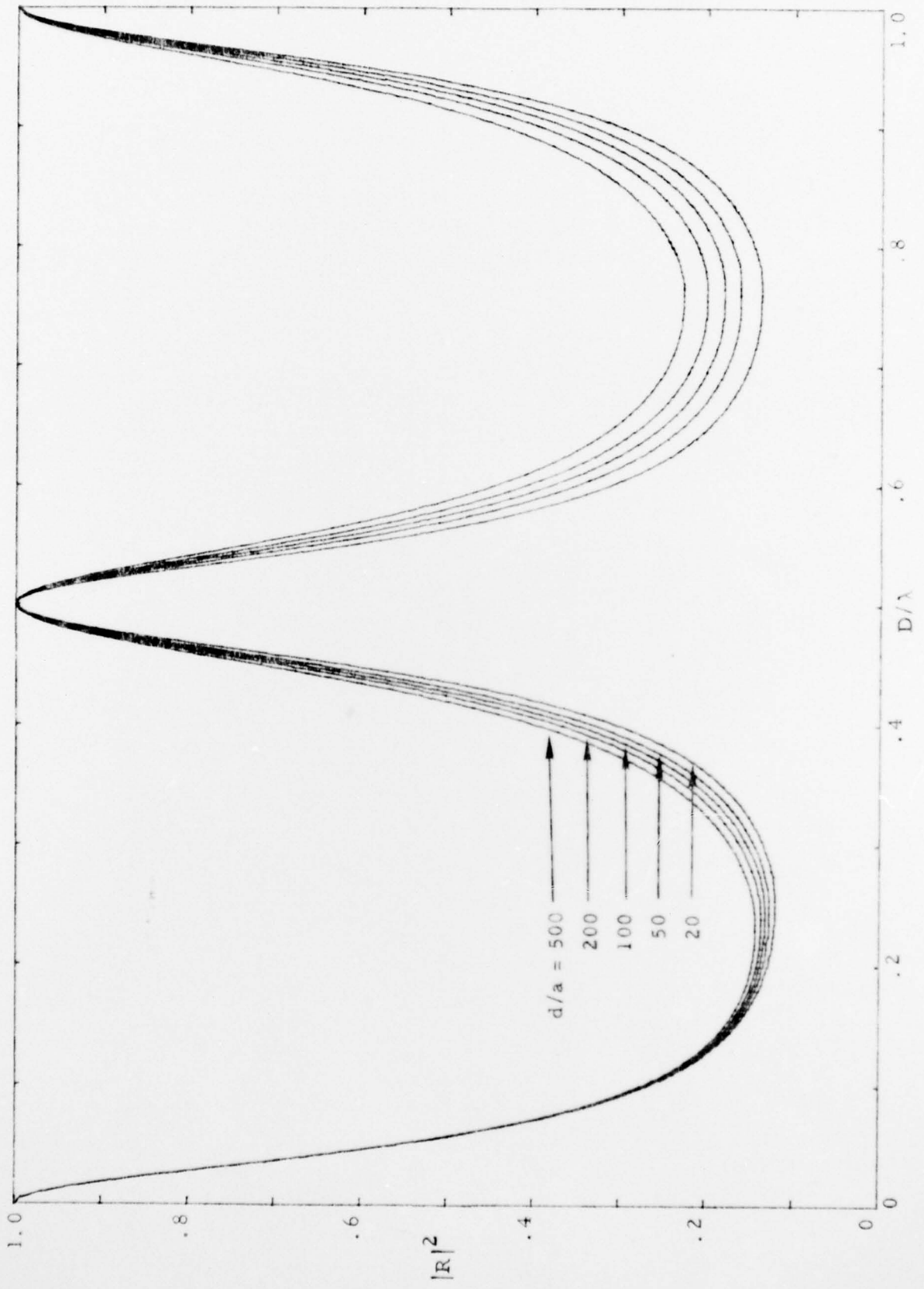


Fig. 20: $|R|^2$ vs. D/λ for $z_r = .5$ and $d/D = .1$

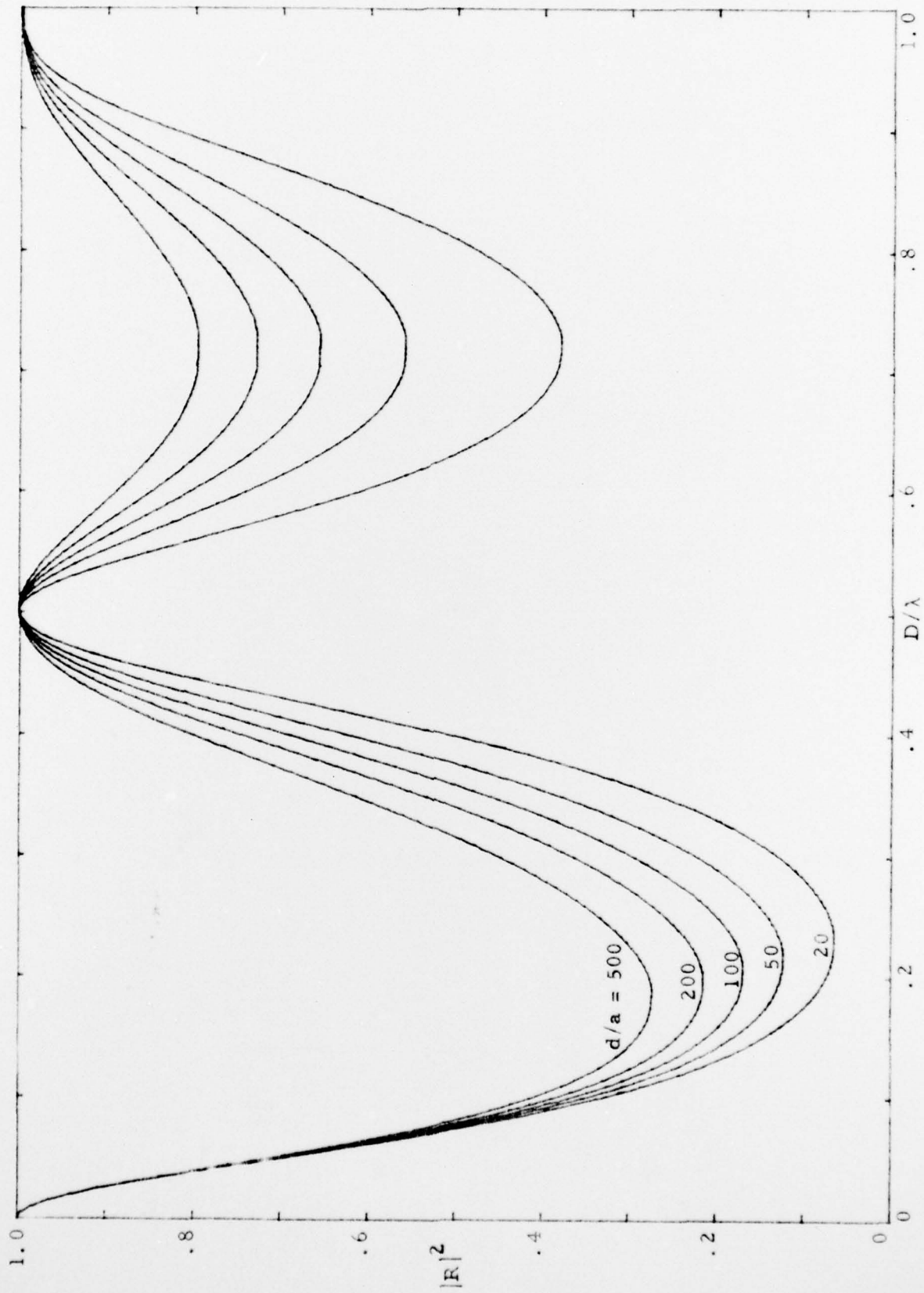


Fig. 21: $|R|^2$ vs. D/λ for $z_r = 1$ and $d/D = 1$

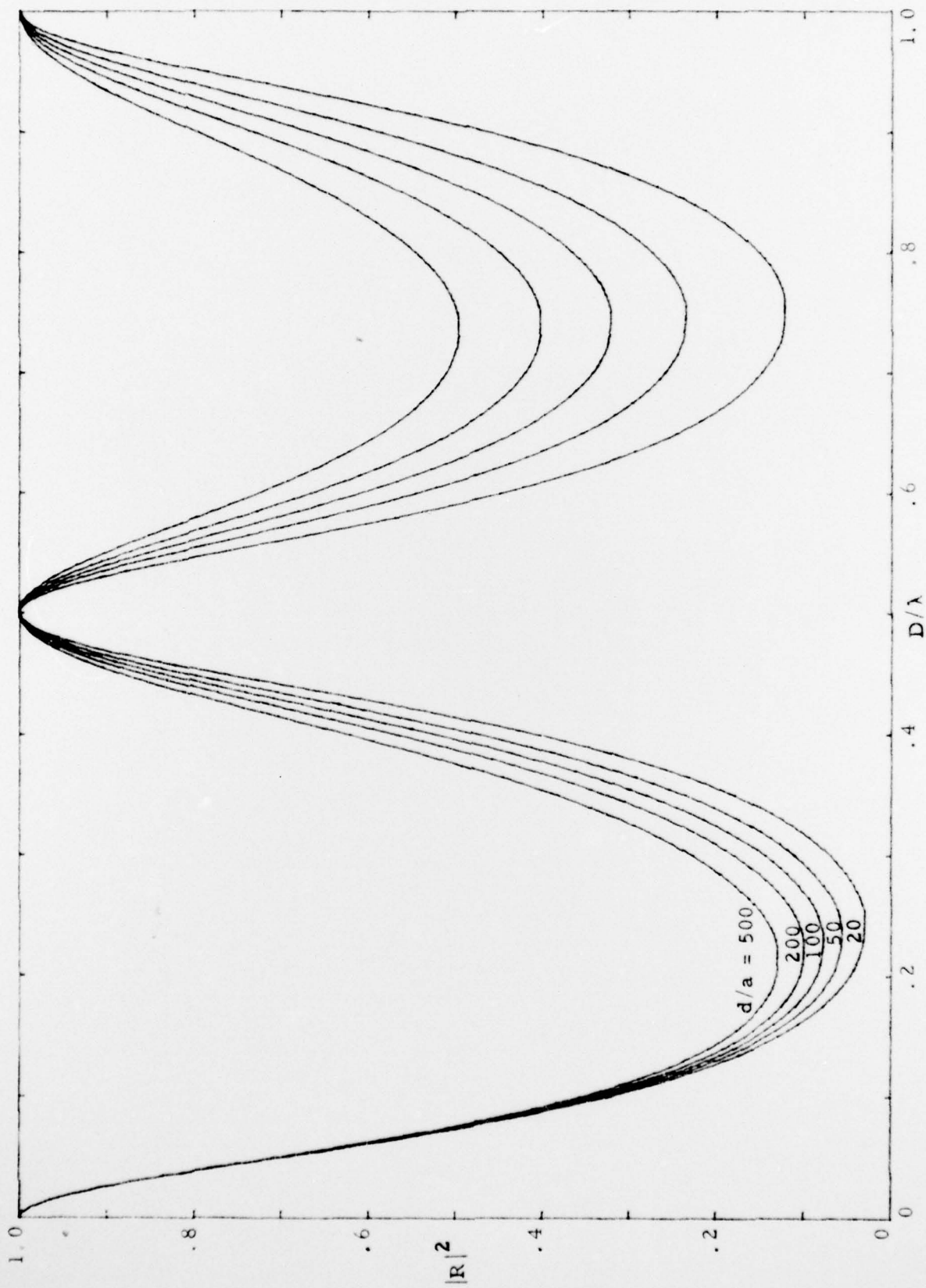


Fig. 22: $|R|^2$ vs. D/λ for $z_T = 1$ and $d/D = .5$

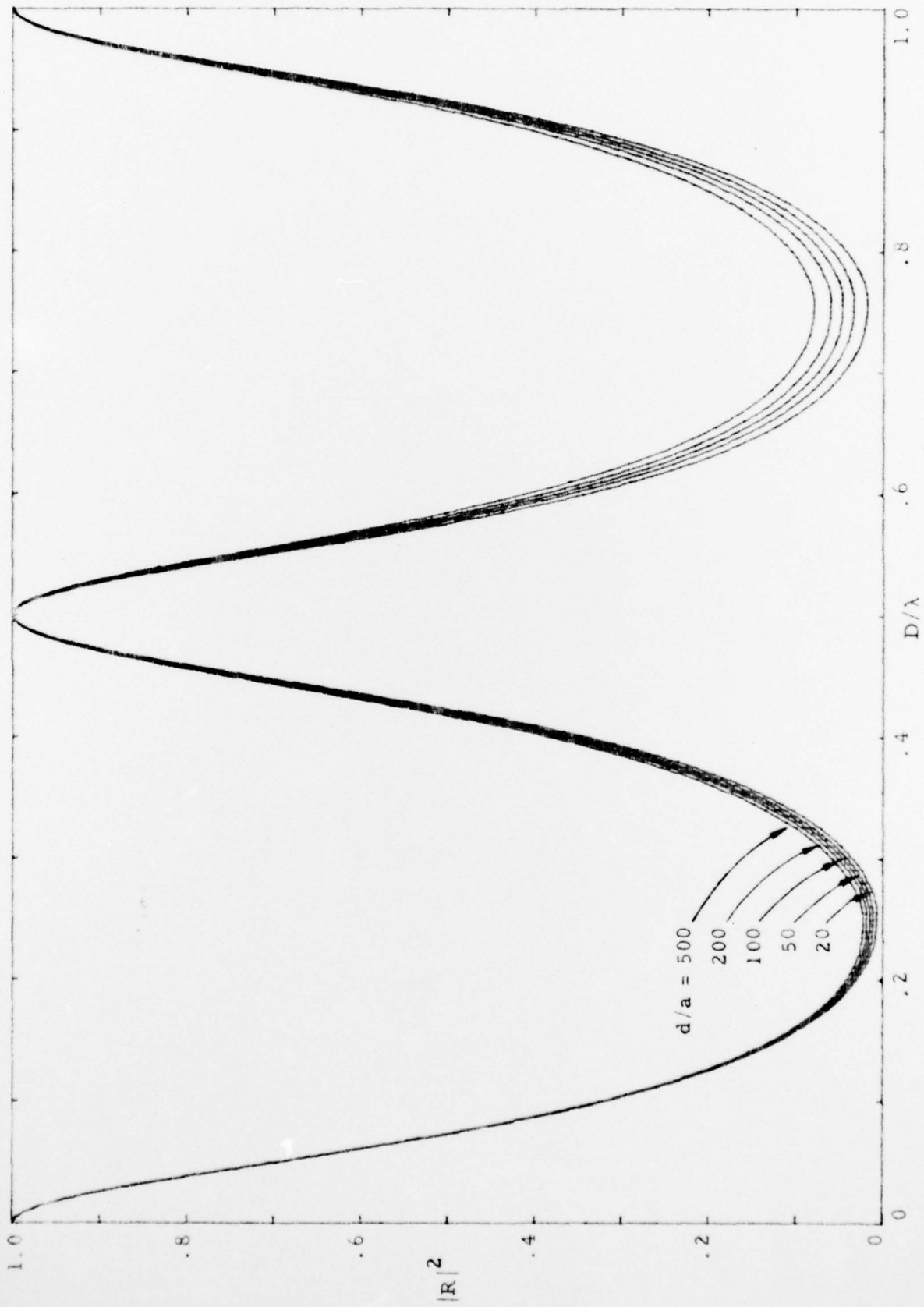


Fig. 23: $|R|^2$ vs. D/λ for $z_T = 1$ and $d/D = .1$

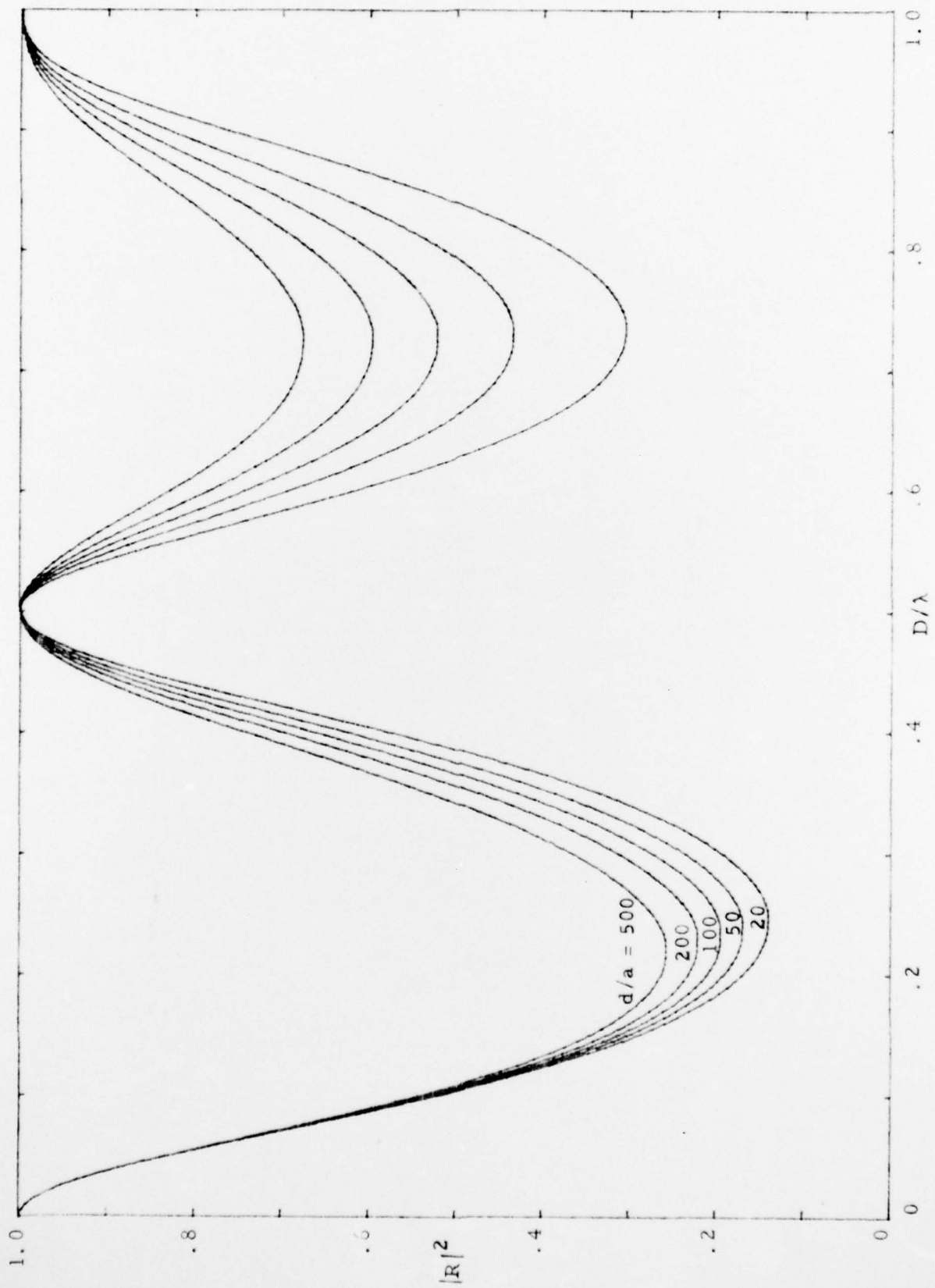


Fig. 24: $|R|^2$ vs. D/λ for $z_r = 2$ and $d/D = 1$

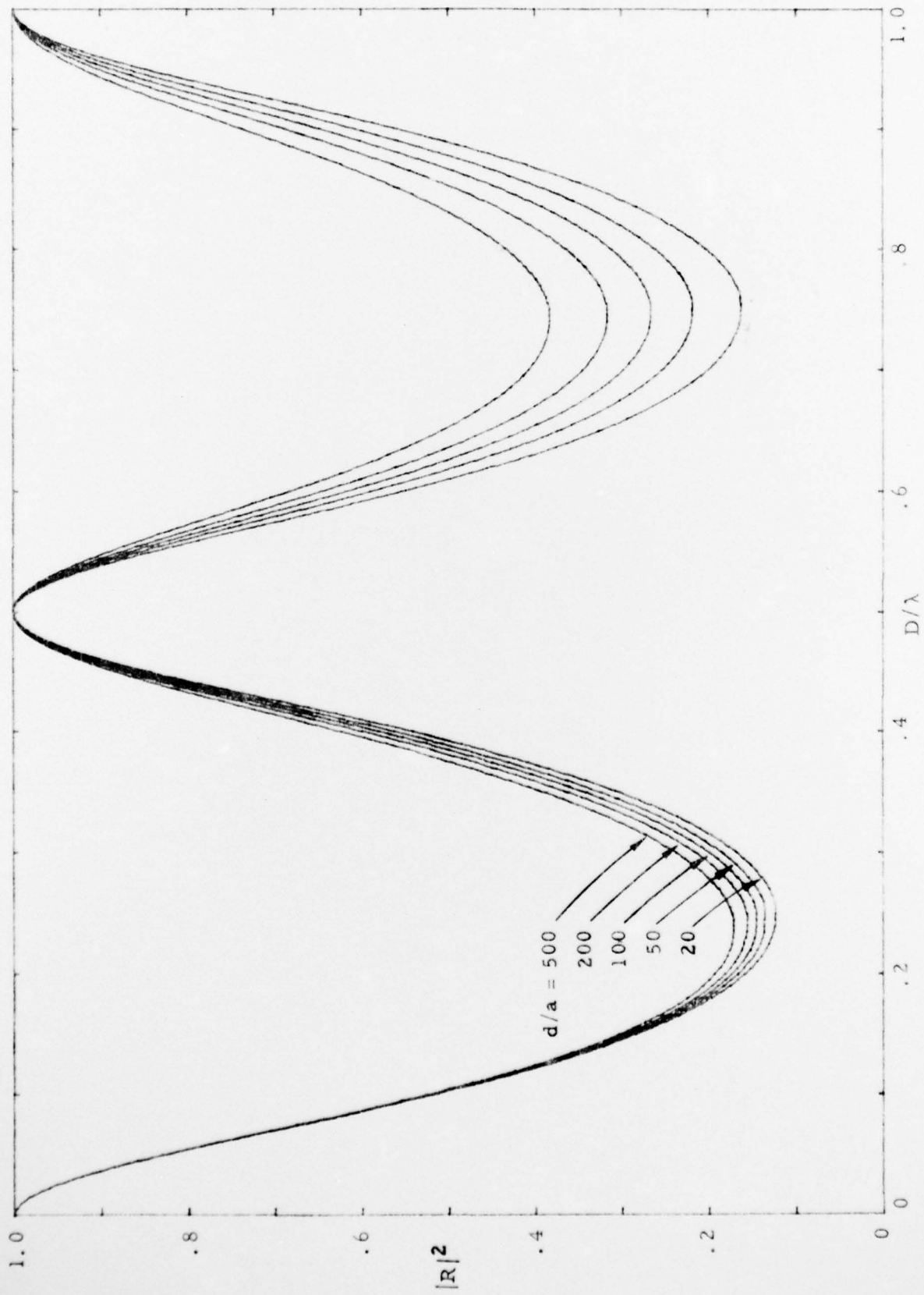


Fig. 25: $|R|^2$ vs. D/λ for $z_r = 2$ and $d/D = .5$

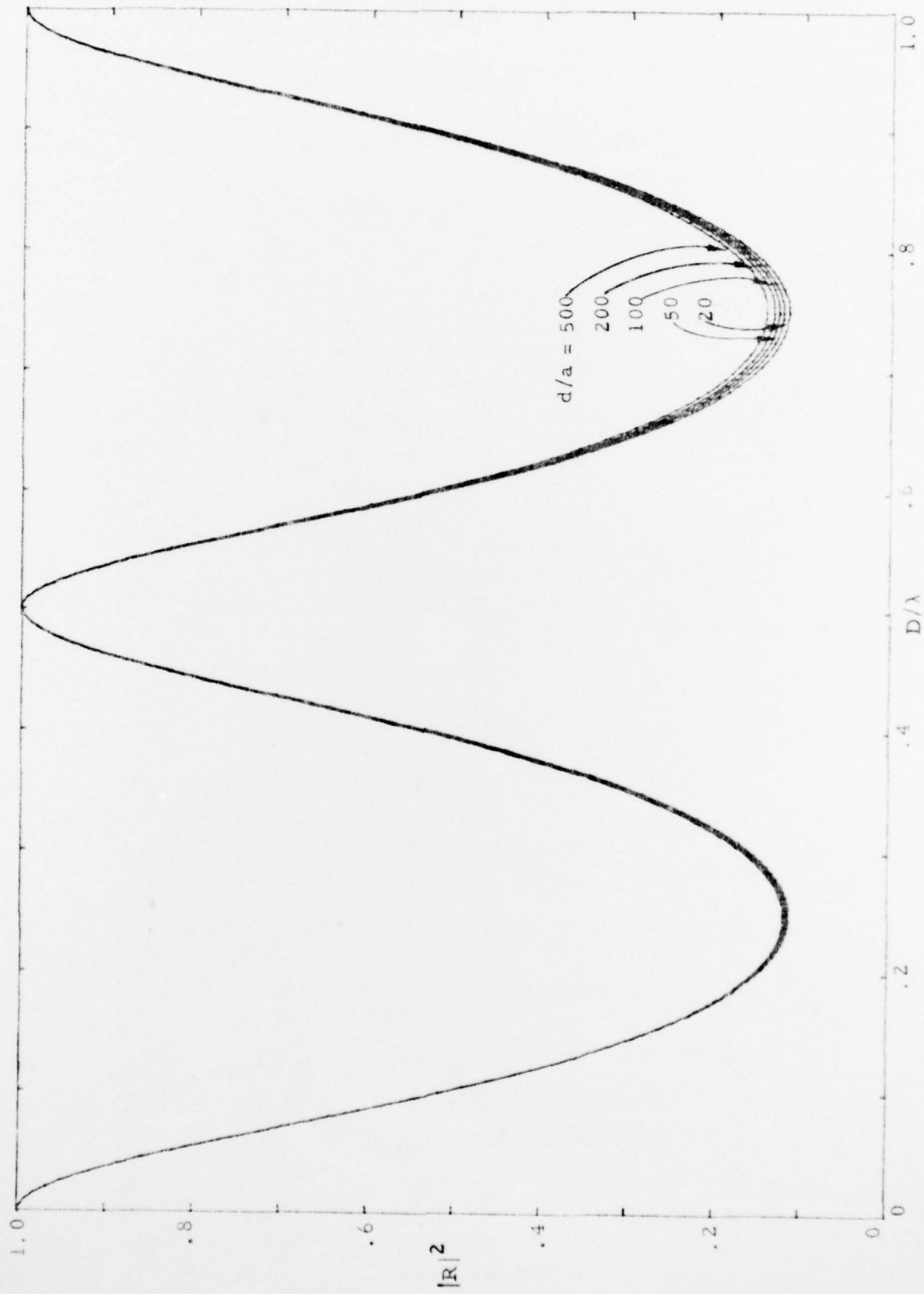


Fig. 26: $|R|^2$ vs. D/λ for $z_I = 2$ and $d/D = .1$

SECTION IV

DISCUSSION

There are several points that can now be made in summarizing the results of Sec. II and by surveying the curves of Sec. III.

1. The resistive sheet that minimizes the average reflected energy over a broad band is the one that has $z_r = 0.707$. With this value of z_r , 31% of the energy is reflected.
2. The resistive sheet that minimizes the energy in the reflected pulse, if the incident pulse is given by $U(t) e^{-t/\tau}$, is the one with

$$z_r = \sqrt{\frac{1}{2} \left(1 - \ell^{-2X_0} \right)}$$

The fraction of the energy reflected is

$$f_{\min} = \frac{2\sqrt{2} - \sqrt{1 - \ell^{-2X_0}}}{2\sqrt{2} + 3\sqrt{1 - \ell^{-2X_0}}}$$

where $X_0 = (D/\tau c)$. f_{\min} is less than $\frac{1}{2}$ for X_0 greater than 0.89. f_{\min} is less than $\frac{1}{3}$ for X_0 greater than 1.1.

3. The resistive sheet that minimizes the fraction of energy reflected at a given frequency, ω_0 , is one with

$$z_r = \sin(\omega_0 D/c)$$

The fraction of the energy reflected at ω_0 is then equal to

$$\frac{1 - \sin(\omega_0 D/c)}{1 + \sin(\omega_0 D/c)}$$

4. One can increase the initial drop-off of $|R|^2$ at low frequency by using small values of z_r (if the sheet is purely resistive). The

price is that $|R|^2$ does not drop very far, just fast.

5. One can create a null in the reflected energy at ω_0 , if $\pi/2 < (\omega_0 D/c) < \pi$, by using a sheet made up of inductance and resistance in series. The appropriate values are $z_r = \sin^2(\omega_0 D/c)$ and $z_i(\omega_0) = \frac{1}{2} \sin(2\omega_0 D/c)$. The null gets sharper the closer it is forced toward π .
6. One can create a null in the reflected energy at ω_0 , if $0 < (\omega_0 D/c) < \pi/2$, by using a sheet made up of capacitance and resistance in parallel. The appropriate values are $y_r = 1$ and $y_i(\omega_0) = -\cot(\omega_0 D/c)$. The null gets sharper the closer it is forced toward 0.
7. A grid of wires with $d/D < .2$ gives energy reflection coefficients differing very little from those for $d/D = 0$ as long as z_r is of order 1 and d/a is less than about 50.
8. A grid of wires with $d/D < .5$ has an energy reflection coefficient different from that for $d/D = 0$ by not much more than .1 if z_r is of order 1 and d/a is less than about 50.
9. The energy reflection curves for $\frac{1}{2} < z_r < 2$ are grouped rather closely together for $D/\lambda < \frac{1}{2}$.
10. The effect of d/a (as long as it is less than about 50) is quite small if d/D is less than about .1.

All in all, if sufficient importance is given to simplicity (i. e. ease of construction) the single-grid reflection reducer could be quite adequate. However, two further factors that must be considered before a final decision on the number of grids can be made are:

1. What we have done throughout this note is to restrict ourselves to frequencies high enough that an infinite planar grid analysis

is adequate. At the lower frequencies, where cavity mode damping may become important, more than one grid may be optimum.

2. If frequencies high enough for D/λ to be of order $\frac{1}{2}$ are important, a second grid could be useful in cutting out the periodic return of $|R|^2$ to unity. This second grid should be placed so that $D_1 \neq D_2$. Perhaps $D_2 \ll D_1$ would be a good choice for both mode damping and destroying the periodicity of $|R|^2$.

REFERENCES

- [1] Carl E. Baum, "A Technique for Simulating the System Generated Electromagnetic Pulse Resulting from an Exoatmospheric Nuclear Weapon Radiation Environment," *Sensor and Simulation Notes*, Note 156, September, 1972.
- [2] G. A. Otteni, "Plane Wave Reflection from a Rectangular-Mesh Ground Screen," *IEEE Transactions on Antennas and Propagation*, Vol. AP-21, No. 6, November, 1973, pp. 843-851.
- [3] James R. Wait, "Reflection from a Wire Grid Parallel to a Conducting Plane," *Canadian Journal of Physics*, Vol. 32 (1953) pp. 571-579.
- [4] R. W. Latham, "Reflection from an Array of Dielectric Posts," *Sensor and Simulation Notes*, Note 180, June, 1973.
- [5] Carl E. Baum, "Impedance and Field Distributions for Parallel Plate Transmission Line Simulators," *Sensor and Simulation Notes*, Note 21, June, 1966.
- [6] I. S. Gradshteyn and I. M. Ryzhik, Table of Integrals, Series, and Products, Academic Press, New York, 1965.